IEEE Access
Multidisciplinary | Rapid Review | Open Access Journal

Received 29 May 2025, accepted 20 June 2025, date of publication 25 June 2025, date of current version 2 July 2025.

Digital Object Identifier 10.1109/ACCESS.2025.3583228

RESEARCH ARTICLE

Battery Energy Storage System Contribution to Primary Frequency Control in Isolated Power Systems

MUHAMMAD ASAD[1,2], GIULIA TRESCA[2], (Member, IEEE), PERICLE ZANCHETTA[2], (Fellow, IEEE), AND JOSE ANGEL SANCHEZ-FERNANDEZ[1], (Senior Member, IEEE)

[1]Department of Hydraulic, Energy and Environmental Engineering, E.T.S.I. Caminos Canales y Puertos, Universidad Politécnica de Madrid, 28040 Madrid, Spain
[2]Department of Electrical, Computer and Biomedical Engineering, University of Pavia, 27100 Pavia, Italy

Corresponding author: Muhammad Asad (m.asad@alumnos.upm.es)

This work was supported in part by the Universidad Politécnica de Madrid under Grant RP2304330031.

ABSTRACT Increased renewable energy penetration into conventional power plants results in significant frequency regulation (FR) problems, particularly at island power systems. To overcome FR problems, an energy storage system plays an important role. Therefore, a battery energy storage system (BESS) is proposed to provide primary frequency control (PFC) for San Cristobal Island hybrid wind diesel power system (WDPS) in this paper. The aim of this paper is to highlight the improvements achieved using BESS and estimate the optimal size of that BESS for San Cristobal WDPS. Therefore, a permanent magnet synchronous generator (PMSG) based variable speed wind turbine (VSWT) with synthetic (droop) control is used, which enables VSWT to release inertia during contingencies. A novel controller tuning methodology, named student psychology-based algorithm (SPBA), is used to optimally tune the BESS with hybrid WDPS and to estimate BESS size. In addition, several configurations set such as BESS with VSWT and/or diesel power plant (DPP) or both, are presented in this paper to highlight the optimal tuning effects. Moreover, the BESS based WDPS is tested under various real-world scenarios such as loss of wind generator, steadily increase wind speed ($\Delta V_w \approx 0.81$ ms^{-1}), variable wind speed, variable load demand (P_{load}) and simultaneously change in V_w and P_{load}. Finally, hybrid BESS based WDPS is tested in a real time environment (OPAL-RT) which validates its performance. Results show the significant reduction in frequency deviation, optimal sizing of BESS and optimal tuning of the whole WDPS.

INDEX TERMS Battery energy storage system, hybrid isolated WDPS, primary frequency control, SPBA, renewable energy, droop control, frequency deviation.

I. INTRODUCTION

Conventional power plants operation changes dramatically, towards a new era of providing electricity and allowing green energy sources to integrate into existing infrastructure, throughout the world [1]. Major reasons that encourage this transformation are reducing dependency on fossil fuels, reduction of greenhouse gas emissions, etc. cite bib:2. Although this adoption (conventional resources-based generation to hybrid renewable based generation) is beneficial in terms of environmental concerns, it also brings some new critical issues to existing power systems, especially for isolated island power systems. One of those critical issues is frequency stability [3]. There are various factors that raise the frequency stability issue. Among them, the major concern is that the intermittent nature of renewable energies (RE), such as wind energy, can result in the imbalance between generation and load demand [4]. This becomes more severe when one of the generating units in an island hybrid power system is lost. Basically, only conventional generators are responsible

The associate editor coordinating the review of this manuscript and approving it for publication was Xiaosong Hu.

for providing inertia (from stored kinetic energy) in hybrid power systems [5]. Because variable speed wind turbines provide negligible inertia due to fast acting power electronics converters between rotor of WT and three phase networks [6]. More precisely, in a wind diesel power system (WDPS) due to any reason or contingencies such as loss of wind generator or increment in load demand, a mismatch between generation and load demand occurred. Then the kinetic energy (K.E) stored in the rotating masses of conventional generators is inherently used to balance such mismatches. But such K.E is not enough to correct it. For this reason, primary and secondary frequency control is needed [7].

Generally, isolated power systems are more sensitive to generation and load imbalances [8]. The reasons behind this sensitive behavior of isolated island power systems are small size and, consequently, low inertial support availability (or K.E) as compared to large, interconnected power systems [9]. Therefore, large generation and load mismatches force the generators to be tripped (if statutory and operational limits are breached). This avoids any physical damage but increases frequency deviations (FD). If frequency excursions (FE) are not within the limits of +-2.5 Hz/s after contingency, then cascade tripping of generators can happen [10]. Author in [11], explain this frequency excursion in a way that: large contingencies may cause unacceptable FE with high FD and rate of change of frequency (RoCoF). This high RoCoF and FD, may initiate an under-frequency load shedding, to arrest the frequency decline. That's why isolated islands, that face high renewable energy penetration, can lose hydro, steam or wind generators synchronism if RoCoF exceeds 2 Hz/s. Consequently, if RoCoF exceeds 3 Hz/s, then under-frequency load shedding relays may fail to respond quickly to shed necessary amount of loads, which eventually results in power systems blackouts [12]. All these reasons justify the significance of primary frequency control (PFC) in power systems, especially in isolated ones. These are the few major reasons that support the future power system concerns, as stated in [13] and [14] "in the future power systems FE is expected to be increased because RE generators replaced the conventional generators (so less available inertia) and fluctuating, variable, less predictable supply of RE". Therefore, PFC is essential to maintain power system stability and reliability [15].

In this paper, the hybrid wind diesel power system (WDPS) of San Cristobal Island, facing critical blackouts due to tripping of frequency relays [16], is considered to provide PFC studies. As mentioned above, conventional generators at isolated island power systems are solely, responsible for providing inertial support. But such support is not always enough to stabilize power systems. In addition, RE integration, especially wind energy, has dramatically impacted on pre-existing conventional electrical networks [17] and this integration impact mainly depends on available system inertia and RE penetration rate [18]. Traditionally, wind turbines (WT) do not provide inertial support [19]. However, it might be possible for WT to contribute (releasing inertia) against contingencies and play its role for PFC. With this aim, authors in their previous studies [20] proposed emulation and inertial control loop for wind turbines which enables WT to provide virtual inertial support during NADIR or contingencies. One of the major advantages of this control is that WT can operate at its optimum operational point (OOP) [21]. Otherwise working at non-OOP has economic effects. These wind turbines are variable speed wind turbines (VSWT) because VSWT have the capability to operate in a wide range of angular velocities against fluctuating wind. Therefore, authors used the hybrid WDPS of San Cristobal Island, in this research for PFC enhancing. The detailed parameters of San Cristobal Island are given in Table 3 and Table 4 (Appendix). However, a detailed information about various aspects of San Cristobal Island electricity sector, total load demand and its type, map etc. presented in literature [16], [22], [23], [24], are out of scope of this study.

To achieve goals of reducing FD and PFC, inclusion of energy storage systems (ESS) is considered. Because ESS has been receiving wide attention from researchers in recent years [25], [26], [27]. Integration of ESS is an effective solution for overcoming RE resources intermittency and fluctuating effects. Furthermore, ESS can provide economic and technical solutions or advantages [28] with increased profitability to various challenges such as grid security, stability, power quality, generators low utilization factors, congestion management and fuel price volatility. Moreover, ESS also provides benefits to the ancillary service market [29] for remuneration in exchange for market benefits (loss prevention, stability enhancement or hedging risk) [30]. Likewise, advancement in technology and increased research and development, the capital cost of battery energy storage systems (BESS) is significantly reduced [31]. This opens new doors to study its applications and economic benefits. That's why BESS is one of the suitable options to support PFC [32]. In case of frequency drop, energy from the battery discharges and vice versa. To perform such regulation (charging and discharging), BESS is well suited because it provides fast response (because of small time constant). Although, the time constant of BESS depends on power conditioning equipment and control, typically, it can be between a few tens of milliseconds to seconds [33], [34]. Additionally, BESS is composed of only static elements, that's why BESS has a fast dynamic response as compared to other storage devices [35]. Some other merits of BESS include environmental compatibility, modularity, high reliability and readily available technology. That's why BESS is adopted for hybrid VSWT based WDPS of San Cristobal Island in this research work.

There are the following objectives of this paper:

1) Enhance the PFC of San Cristobal Island hybrid WDPS with proportional control loop and BESS. It means, whenever contingencies happen DPP, VSWT and BESS (by charging/discharging), simultaneously provide inertial support to restore the power system to its initial state by reducing NADIR. A detailed discussion about the role of BESS is made in Section IV and VI.

2) Provide optimized sizing of the BESS for San Cristobal Island hybrid WDPS with exhaustive search. Additionally, a detailed comparison of various situations such as a) Case X: simultaneously optimized BESS and VWST with fixed parameters of DPP b) Case Y: simultaneously optimized BESS and DPP without changes in VWST c) Case Z: simultaneously optimized all three systems (DPP + VSWT + BESS).
3) Provide global optimized parameters of hybrid BESS based VSWT WDPS using Student Psychology Based Algorithm. In addition, a comparison and effects of various tuning methodology such as Ziegler- Nicolos and MATLAB auto tuning with SPBA. Such comparison highlights the pros of SPBA.
4) Moreover, hybrid BESS based WDPS performance is tested under various sets of real contingencies to justify its behavior and efficacy. Real world contingencies include a) sudden loss of wind generator/load demand increment b) steadily increased in V_w ($\Delta V_w \approx 0.81$) c) wind speed variations while load demand stable d) load variations while V_w varied e) simultaneously variation in both V_w while P_{load})
5) Finally, tested the WDPS performance under a real time (OPAL-RT) environment irrespective of traditional testing. Therefore, developed an emulation of voltage and current based model of San Cristobal Island hybrid BESS based WDPS and tested it in real time.

This paper is organized as follows: diesel power plant and wind turbine modeling are presented in Sections II and III. Section IV presented the modeling of battery energy storage systems. Section V shows the detailed methodology of proposed control i.e., Student Psychology based Algorithm (SPBA). Detailed simulations and results, including contingency effects, is presented in Section VI. BESS sizing is discussed in Section VII. The performance of proposed controllers is analyzed in Section VIII. Real-time simulation results are presented in section IX and, finally, conclusions are outlined in Section X.

II. DIESEL POWER PLANT (DPP) MODELING

Diesel Power Plant comprises conventional diesel generator (DG) in which diesel engine is used as prime mover to produce electrical energy using diesel as a fuel. Traditionally, electricity on isolated islands is produced using DPPs [36]. In addition, a DPP can provide inertial support during contingencies by releasing kinetic energy (KE) from its rotor masses [37]. However, with the integration of RE with conventional DPP, overall inertial support of the power system is reduced [38]. Therefore, to highlight the effects of inertial support, San Cristobal Island DPP is considered in this study. Detailed modeling of DG has already been developed by authors in their previous work [39]. However, the general schematic of DG is shown in Figure 1. It is important to mention that DG requires a proper control system for its operation because it is an unstable electromechanical machine [40]. Figure 1 shows that DG prime mover (PM) is composed of four components i.e., actuator (control the fuel flow in PM), speed governor (control the diesel engine actuating on incoming fuel rate), crankshaft dynamics (convert the reciprocal motion of the piston into rotatory motion) and diesel engine or combustion system (convert fuel energy into shaft mechanical energy). Here, t_m, t_e, represent mechanical torque and torque opposed by electrical generators respectively. Similarly, H_t represents inertia constant and t_1, t_2 and t_3 represent time constants. The detailed parameters of DPP are given in Table 3.

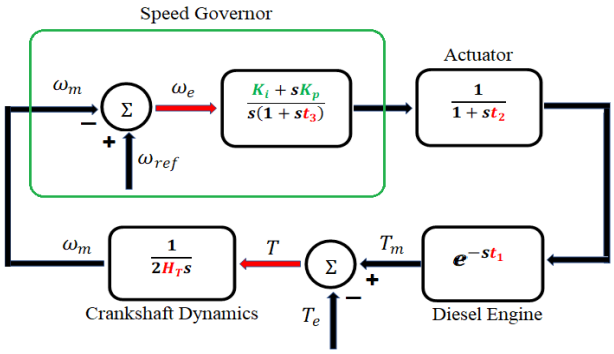

FIGURE 1. Schematic block representation of DG (CAT-3512 DITA) PM.

III. VARIABLE SPEED WIND TURBINE (VSWT) MODELING

Like DG, WT is also an electro-mechanical device. However, instead of using diesel, WT used wind energy to produce electrical energy. This paper considers Type 4 PMSG based VSWT as shown in Figure 2. It is worthwhile to mention that authors developed a DFIG based VSWT model in a previous work [6], [20]. However, this model can be applied for PMSG based VSWT via full converter due to the similarities between their mechanical topologies and because, within the time frame considered in the load frequency control studies, the electromagnetic time constants are negligible compared to the mechanical ones [16]. This simplified WT model has four components i.e., aerodynamics model (harness the wind energy), mechanical model (combination of mechanical system and gear box), converter model (composed of two back-to-back power electronics converters having a DC link) and generator system (composed of PSMG). It is important to mention that the converter model enables PSMG to operate within a wide range of speed variations. In addition, this model doesn't allow WT to contribute inertial support or release KE against contingencies because fast-acting power electronics converters decouple electric machine from the grid. Before discussing emulation inertial and proportional control, authors briefly describe the mathematical representation of WT various components. Equation (1) represents the WT power ($P_{t[p.u]}$) extracted from the wind.

Here, $P_{base[W]}$, V_w, C_p, λ, β and R represent the turbine base power (W), wind speed (m/s), turbine power coefficient, relative turbine speed, blade angle (degrees), air density (kg/m^3) and turbine radius (m). Equation (1) clearly shows

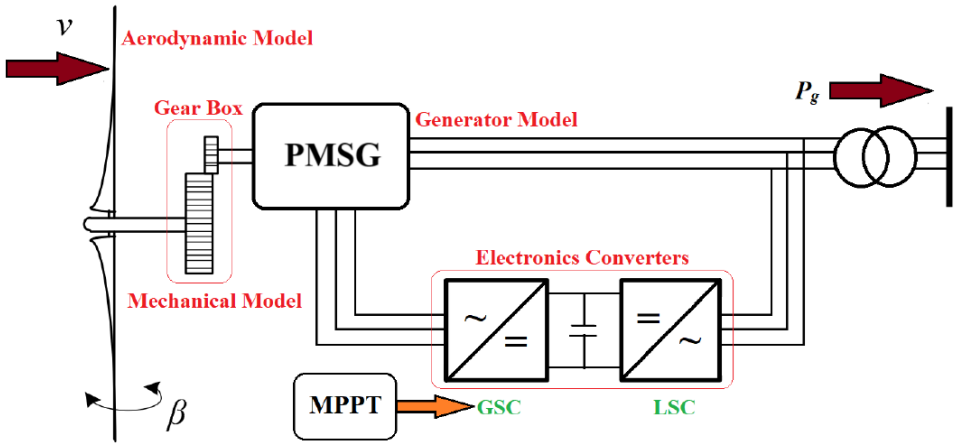

FIGURE 2. General schematic of VSWT.

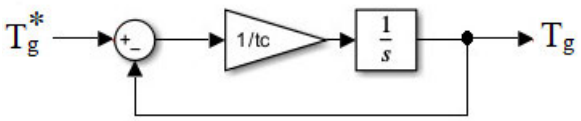

FIGURE 3. Synchronous generator and power electronic converters of VSWT.

that turbine power coefficient (ratio of extractable mechanical power to the power in wind [41]), depends on λ (ratio of WT rotor blade tip speed and wind speed) and β. Therefore,

$$P_{t\ [p.u]} = \frac{1}{2}\frac{\rho\pi R^2}{P_{base,[W]}} V_w^3 C_p(\lambda, \beta) \tag{1}$$

where,

$$C_p = c_1\left(\frac{c_2}{\lambda_i} - c_3\beta - c_4\right)^{-\frac{c_5}{\lambda_i}} + c_6\lambda \tag{2}$$

$$\frac{1}{\lambda_i} = \frac{1}{\lambda + 0.08\beta} - \frac{0.035}{\beta^3 + 1} \tag{3}$$

$$\lambda = \frac{\omega_{t,\text{base[rad/s]}} D_{(m)} K_v \omega_{t[p.u]}}{2V_{w[ms-1]}} \tag{4}$$

Here, $\omega_{t,base}$, $\omega_{t,[p.u]}$ and D are base turbine rotor speed (rad/s), turbine rotor speed (per unit) and turbine diameter (m) respectively.

Similarly, other components of wind turbine are (1) generator and power electronics converter (Figure 3), (2) blade pitch angle control (BPAC), (3) maximum power point tracking (MPPT), given in Equation (6), (4) mechanical system (Equation (5)). So, t_c, t_p, T_g^*, T_g, T_t and H_i represent the time constant of 1st order actuator, servomotor time constant, torque generated by speed controller, converter demanded torque, turbine generated torque and inertial constant of turbine, respectively.

As previously mentioned, WT itself does not contribute to PFC because the non-optimal operation of WT [21] inevitably leads to economic losses [42]. However, authors introduced new emulation and inertial loop (K_{pn} and K_{dn}) in their previous research to enable WT to release synthetic inertia [20]. Here, K_{pn} provides fast frequency response (FFR) while K_{dn} delivers support in RoCoF. However, in that previous research [20] authors concluded that droop control is a better alternative to emulation inertial and proportional control as shown in Figure 4. It provides nearly the same support compared to its combination with inertial control. Therefore, authors prefer to use droop control, which further simplified the model. Moreover, BPAC of VSWT are also modified by introducing a PI control having gain parameters (K_{pc} and K_{ic}) to provide pitch compensation [21], [43], as shown in Figure 5.

$$\frac{d\omega_t}{d_t} = \frac{\Delta T}{2H_i} \tag{5}$$

$$P_g^* = \begin{cases} \dfrac{(\omega_g - \omega_{\min})}{(\omega_0 - \omega_{\min})} K_{opt}\omega_0 & \omega_{min} \le \omega_g \le \omega_0 \\ \omega_g^3 K_{opt} & \omega_0 \le \omega_g \le \omega_1 \\ (\omega_g - \omega_{\max})\dfrac{P_{max} - K_{opt}\omega_1^3}{(\omega_{max} - \omega_1)} + P_{max} & \omega_1 < \omega_g < \omega_{max} \\ P_{max} & \omega_g \ge \omega_{max} \end{cases} \tag{6}$$

IV. MODELING OF BATTERY ENERGY STORAGE SYSTEM

A battery energy storage system (BESS) is used in this study to contribute to primary frequency regulation (PFR). The aim of PFR is to maintain the power system frequency within a pre-defined interval against contingencies or imbalances between generation and load [44], [45]. The BESS model used in this study is described in [46] and [47] as a first order transfer function given by Equation (7). Here, Δf is the frequency deviation (p.u.), K_{bess} is the droop control or gain, T_{bess} is the BESS time constant (it ranges vary between tens of seconds to seconds [46]) and P_{bess} is the output power

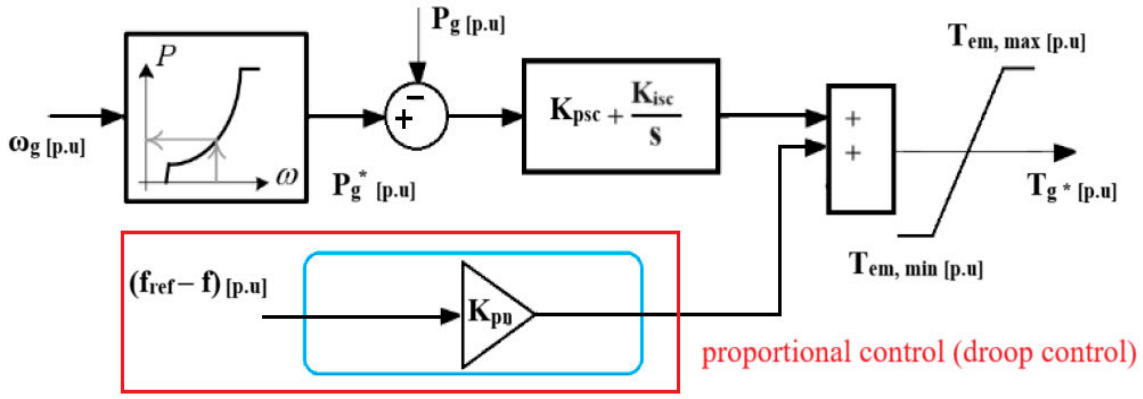

FIGURE 4. Synthetic inertial support control (droop control) of VSWT.

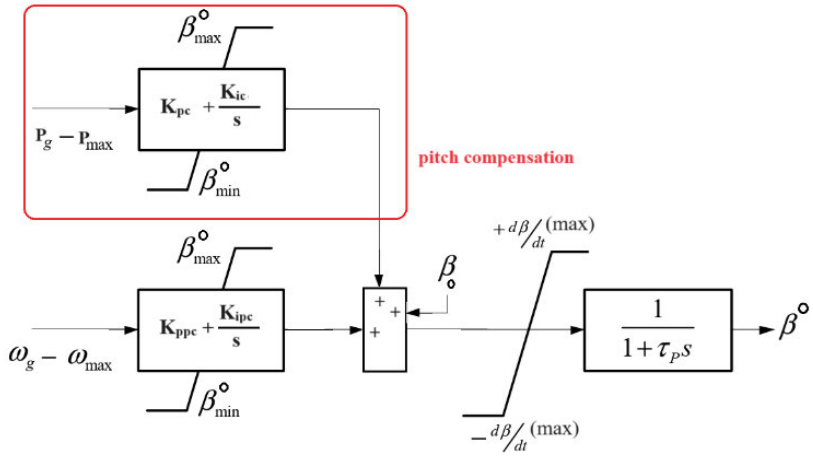

FIGURE 5. BPAC with pitch compensation.

of BESS (p.u). The MATLAB schematic of BESS is shown in Figure 6. It clearly shows that the input of BESS is the difference of frequency (i.e., nominal frequency and actual frequency of conventional generator). Therefore, BESS can supply or absorb energy during contingencies. The impact of the BESS on hybrid WDPS is explained in the following sections. In addition, the BESS sizing for San Cristobal Island power system is presented in Section VII.

$$\frac{\boldsymbol{P_{bess}}}{\boldsymbol{\Delta f}} = \frac{\boldsymbol{K_{bess}}}{\boldsymbol{1 + st_{bess}}} \tag{7}$$

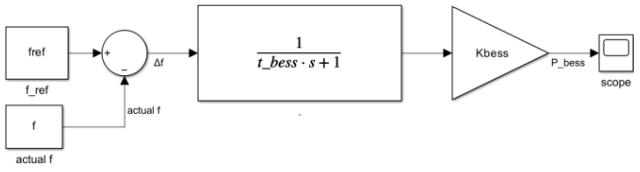

FIGURE 6. Proposed BESS for VSWT hybrid WDPS of San Cristobal Island.

V. STUDENT PSYCHOLOGY BASED ALGORITHM

SPBA is used in this study for controller tuning which authors developed in their previous work [39]. However, authors briefly discussed it below, to justify its usefulness and importance for this research study. Basically, SPBA performs based on controller quality index Z, given in Equation (8). Here, ISE, IAE, NADIR and c represent integral square error, integral absolute error, under frequency (p.u) and number of sign changes in frequency derivatives during contingencies. It is important to mention that finding a group of controller's gains parameters that jointly provide the best values of all above-mentioned objective functions or indicators is very difficult. Therefore, the authors proposed a coefficient, Z with aim to achieve a compromising solution that improves all the above-mentioned quality indicators or objective functions at the same time. The general schematic of SPBA for a PI controller (having gain parameters K_p and K_d) is shown in Figure 28 (Appendix). However, it is important to mention that SPBA can be extended to more than one controller at a time, to obtain optimal results. It is clearly shown that variables in Figure 28 are two (K_p and K_d). Therefore, the

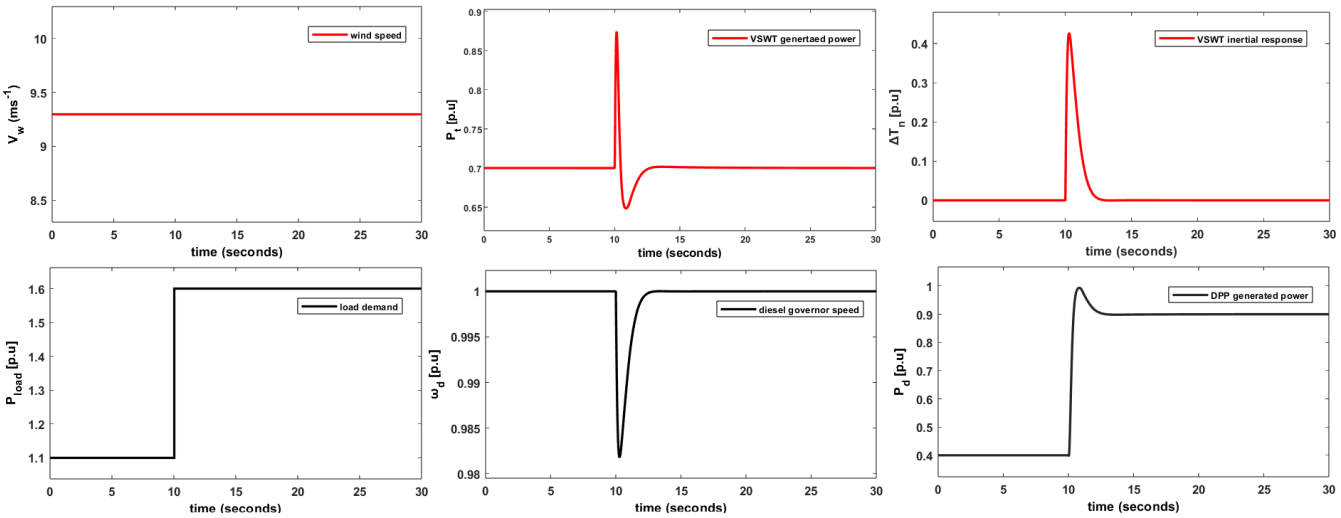

FIGURE 7. Results of various parameters under base case of hybrid VSWT WDPS without BESS.

maximum possible combinations of K_p and K_d trends are eight, out of them only one is the best path for optimal solution. SPBA starts with the base gain parameters ($K_{p,base}$ and $K_{d,base}$) of PI controller under study. Firstly, all the parameters of controller quality index (Equation (8)) are calculated according to the base gain parameters of PI controller and stored in vector V_a. After that, increments and decrements in the values of K_p and K_d are executed, according to eight different possibilities. SPBA calculates controller quality index values against each possibility and compares it with Z_{base}. If the new Z value is higher as compared to Z_{base} then Z of that combination will be replaced as Z_{new} otherwise return zero. All results of controller-quality indexes are stored in vector $\mathbf{Y}$. Now, there are only two possibilities of Y whether Y is non-zero vector or null vector. In case of non-zero, then SPBA returns greater Z by comparing all elements of $\mathbf{Y}$. Reason for greater Z selection is that greater Z reflects reduced FD or NADIR, lowest ISE and IAE and reduced number of sign changes in frequency derivatives. Therefore, all parameters in $\mathbf{Y}$ are compared with each other with the aim to get highest Z. All parameters against this Z_{new} become base values and repeat this process again until Y returns to zero. If $\mathbf{Y}$ is zero, then the first increment after decimal applied until algorithm again returns zero in $\mathbf{Y}$. It means that algorithm generates optimal solution up to numerical values (without decimal). However, to precise results till 2^{nd} decimal place, an increment in the last selected gain parameters is applied again. Obtaining precise results for up to two decimals is enough because furthermore there is no significant improvement shown in results. Finally, after the increment of up to two decimal places, when $\mathbf{Y} = [\mathbf{0}]$ and $Z_{new} < Z_{prev}$, then SPBA stops. All parameters against Z_{prev} contain optimal results of that controller. Therefore,

- SPBA provides optimal gain parameters for the controller under study.
- SPBA provides minimum NADIR, ISE and IAE.
- SPBA reduces the number of sign changes in frequency derivatives.
- If the values of gain parameters are increased or decreased from optimal solution, then results become worse in terms of increased oscillations, FD and settling time.

$$Z = \frac{NADIR}{ISE * IAE * n} \tag{8}$$

VI. SIMULATIONS AND RESULTS

This section presents various scenarios of BESS with VSWT and DPP to highlight the pros and cons.

A. BASE CASE: VSWT HYBRID WDPS WITHOUT BESS

This case VSWT based hybrid WDPS without BESS is considered as the base case to highlight the significance and improvement in results (discussed below). It is important to mention that the WDPS used in this study as base case is optimally tuned (authors developed it in a previous work [20]). As discussed above, naturally VSWT itself cannot provide any support against FD. Therefore, to make it possible, a droop or proportional control is introduced in VSWT which enables it to release synthetic inertia during contingencies. It concludes that both DPP and VSWT contribute to providing inertial support. However, DPP is the major contributor to restore system NADIR. To find the base parameters of this study, a perturbation of 0.5 p.u as a step response with constant wind speed of 9.2966 ms^{-1} is considered, which reflects the sudden increase in load demand due to the loss of one of the wind generators. Figure 7 clearly shows the behavior of hybrid WDPS. Against 0.5 pu increased in step response, NADIR is 0.9818 p.u (49.09 Hz), IAE is 0.0169 and ISE is 2.0568×10^{-4}. Table 1 shows the base parameters of hybrid WDPS without energy storage. In addition, the contribution of VSWT to provide synthetic inertia is clearly observed in

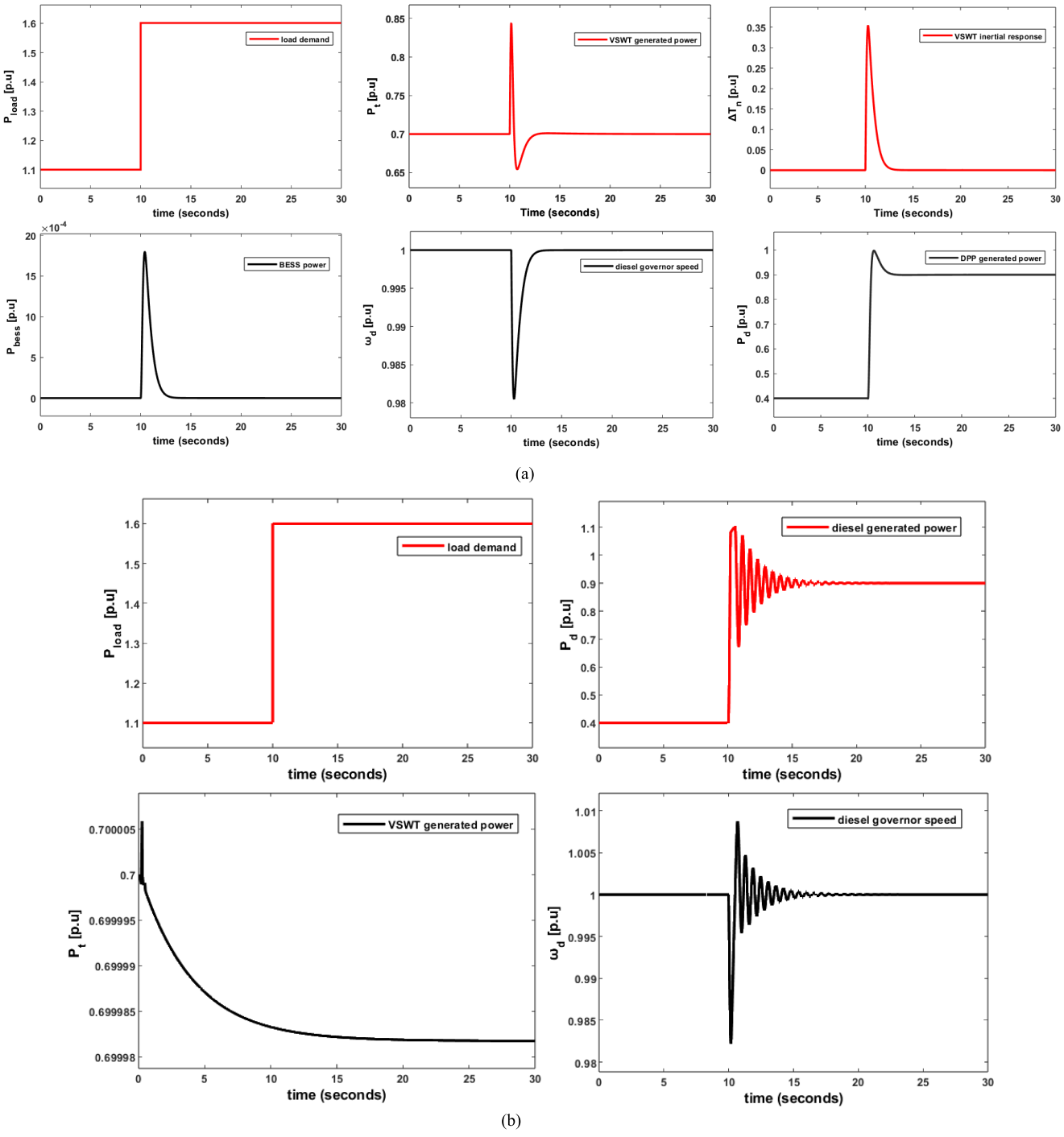

FIGURE 8. **(a): Simulations of hybrid BESS based VSWT WDPS with fixed DG parameters (b): Simulations of hybrid WDPS using Ziegler Nicolos with fixed wind speed.**

Figure 7. Furthermore, to highlight the significance of BESS and its impact with DPP and/or VSWT, following cases are discussed. Table 2 shows the detailed gain parameters of controllers under study.

Before discussing the following cases (Case X, Case Y and Case Z) it is important to mention the relationship between DPP, VSWT and BESS. In hybrid WDPS both power plants are operational according to the relationship given by Equation 9. It means DPP is responsible for providing the difference of power i.e., load demand (P_{load}) and power provided by VSWT (P_t). In hybrid WDPS, wind power plants are integrated into the power system with the aim of providing maximum green generation up to 1 p.u. while DPP is responsible for fulfilling the load demand. However, during

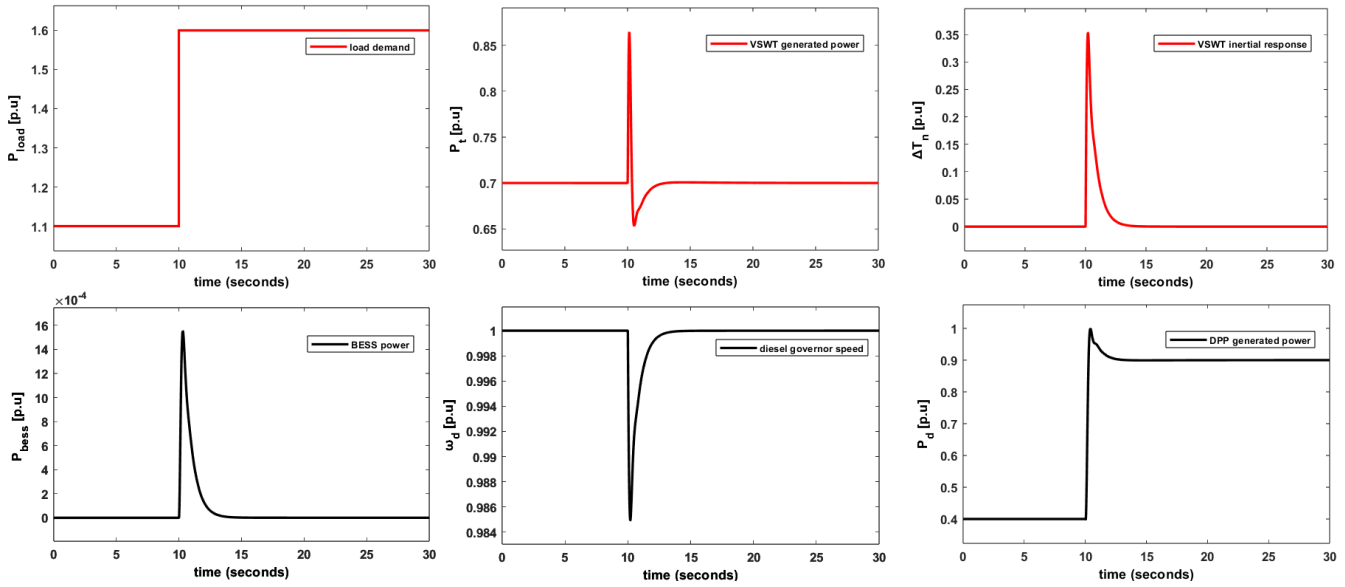

FIGURE 9. Simulations of hybrid BESS based VSWT WDPS without changes in synthetic control of VSWT.

TABLE 1. Hybrid BESS based WDPS tuned parameters.

Case	BESS gain parameter	Diesel governor controller gains parameters		VSWT synthetic (droop) control
#	K_{bess}	K_{p_d}	K_{i_d}	K_{pn}
Base	0	24.65	29.55	23.43
X	0.1	24.65	29.55	18.15
Y	0.12	38.05	43.56	23.43
Z	0.6	46.92	60.31	35.28

TABLE 2. Detailed experimental measurements of Cases base, X, Y and Z.

Case	NADIR (p.u)	ISE	IAE	Z (p.u)
Base	0.9818	2.0568×10^{-4}	0.0169	2.82451×10^{5}
X	0.9805	1.798×10^{-3}	0.0169	3.2267×10^{4}
Y	0.9849	9.4127×10^{-5}	0.0115	9.09871×10^{5}
Z	0.9878	5.6173×10^{-5}	0.0083	2.11866×10^{6}

contingencies both power plants are responsible for providing PFC (latter discussed in the following cases). Moreover, BESS is included in hybrid WDPS solely for PFC. Whenever, any contingencies occur (Δf) BESS will supply or absorb power (by charging or discharging) to minimize NADIR. It is concluded that in hybrid WDPS of San Cristobal Island DPP is responsible to fulfilled variation in load demand while all power systems (DPP+ VSWT+BESS) actively play its role for PFC. It is noted that DPP and VSWT both fulfilled the load demand, but DPP is also responsible to fulfill the variation in load demand when VSWT generates constant power at constant wind speed (Figure 16). The following cases (X, Y and Z) and Section VIII validate the above-mentioned statements in a more detailed manner.

$$P_{load[pu]} = P_{t[pu]} + P_{d[pu]} \tag{9}$$

B. CASE X: VSWT HYBRID BESS BASED WDPS WITHOUT CHANGES IN DPP

In this case, a BESS (Section IV) is introduced to improve the PFC in hybrid WDPS. In this case, both synthetic control (droop control) in VSWT and BESS control are simultaneously tuned using SPBA (discussed in Section V) with the aim to provide PFC during contingencies. It is important to mention that diesel governor parameters (K_{p_d} and K_{i_d}) are unchanged because this case features the impact of BESS with VSWT. However, all three systems, i.e., DPP, VSWT and BESS, contribute to providing support for FD. Figure 8 (a) clearly shows that BESS will provide support during NADIR, against step response of 0.5 p.u. Therefore, NADIR, IAE and ISE are 0.9805 p.u (49.025 Hz), 0.0169 and 2.1037 $\times$ 10^{-4}. While comparing it with base case, results are not effective in terms of improvement i.e., NADIR ($-$0.065 Hz). The reason is that DPP and VSWT were optimally tuned using SPBA. As mentioned before, DPP is the major contributor to reduce NADIR. Therefore, individual tuning of BESS without any changes in DPP is not worthwhile. Table 2 shows the detailed gain parameters of controllers under study.

C. CASE Y: SIMULTANEOUSLY TUNED DPP AND BESS

In this case, authors, simultaneously, optimally tuned considered the DPP and BESS while considering VSWT droop control parameters unchanged. In this case, again considering SPBA and a step response of 0.5 p.u. Figure 9 clearly shows

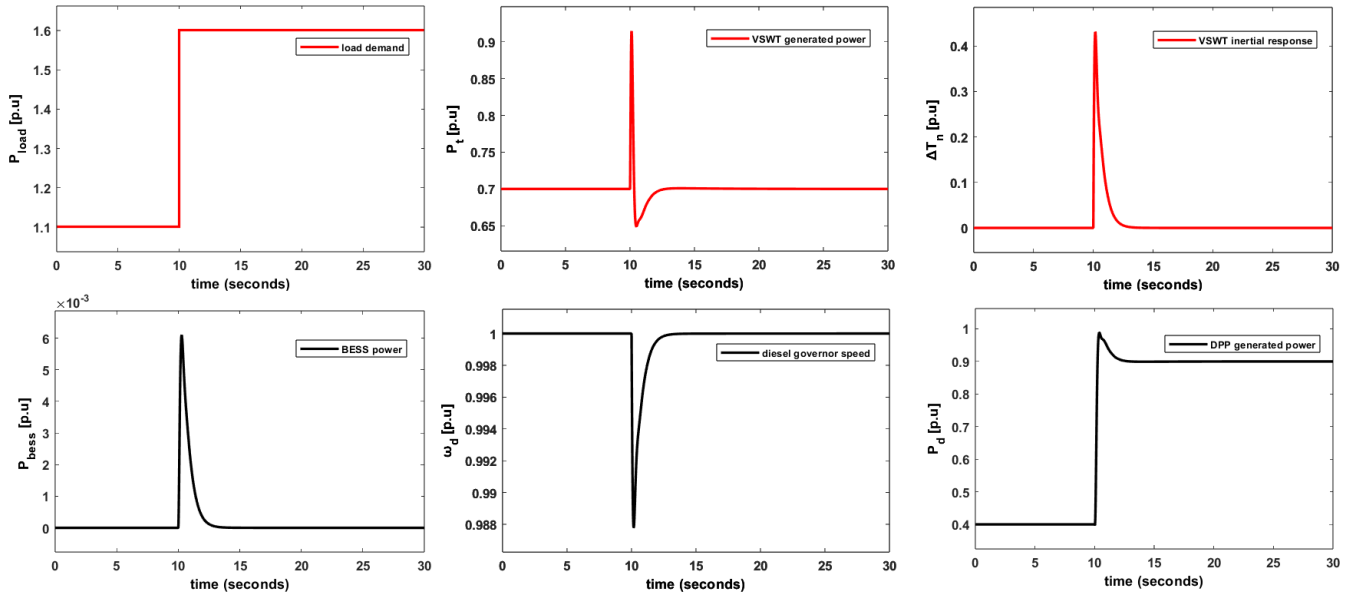

FIGURE 10. Simulations of hybrid BESS based VSWT WDPS against global tuning.

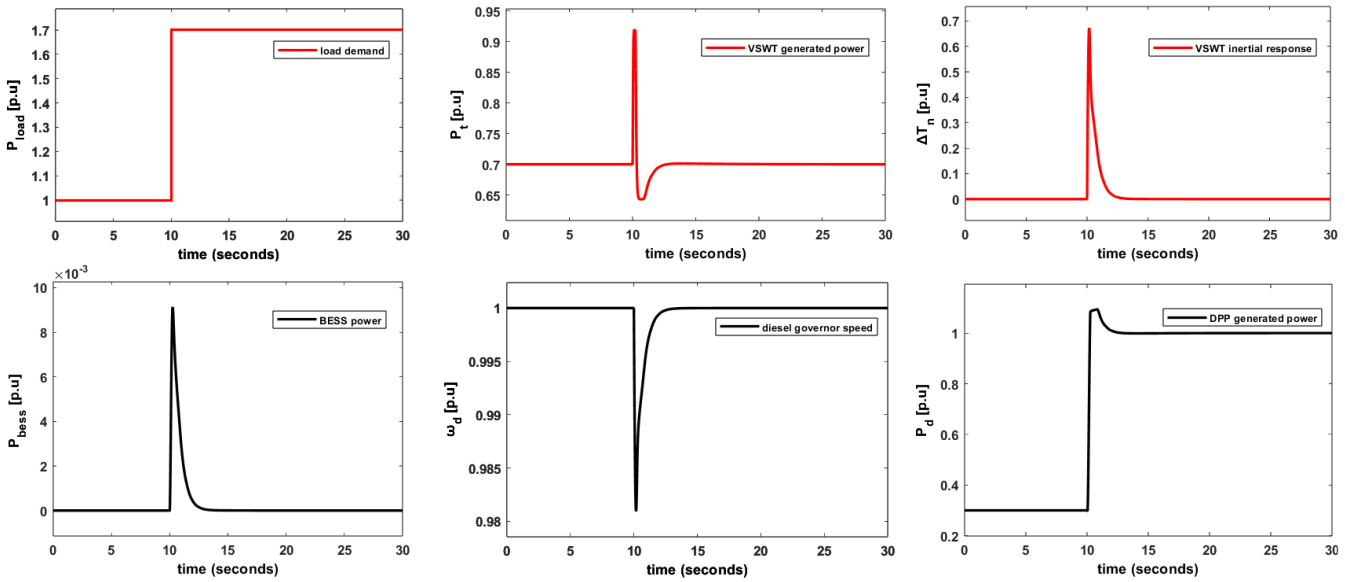

FIGURE 11. Simulation results of hybrid BESS based VSWT WDPS against 0.7 p.u, sudden increase in load demand.

that NADIR significantly improved by 0.315% (0.155 Hz) and 0.447% (0.22 Hz) as compared to base case and case X. In addition, ISE and IAE also improved. Furthermore, VSWT and BESS contribution highlights the effectiveness of inertial support. Table 2 shows the detailed gain parameters of controllers under study.

D. CASE Z: SIMULTANEOUSLY TUNED DPP, VSWT AND BESS

In this case, authors considered the hybrid system as a whole and optimally tuned it to get more effective results. All gain parameters of DPP, proposed synthetic control and BESS are tuned simultaneously, to get global optimal parameters. Figure 10 shows the various effective results of hybrid BESS based WDPS. NADIR, IAE and ISE improved by 0.607% (0.3 Hz), 103 % (0.0086) and 266.07% (1.49×10^{-4}) as compared to base cases. While comparing Case Z with Case Y and Case X, then NADIR is reduced by 0.365 Hz and 0.145 Hz, respectively.

In general, it is concluded that Case Z > Case Y> Base Case > Case X, in terms of providing PFC by reducing FD during contingencies.

Furthermore, Case Z is the best case that represents the global optimal behavior of all three power plants. Therefore,

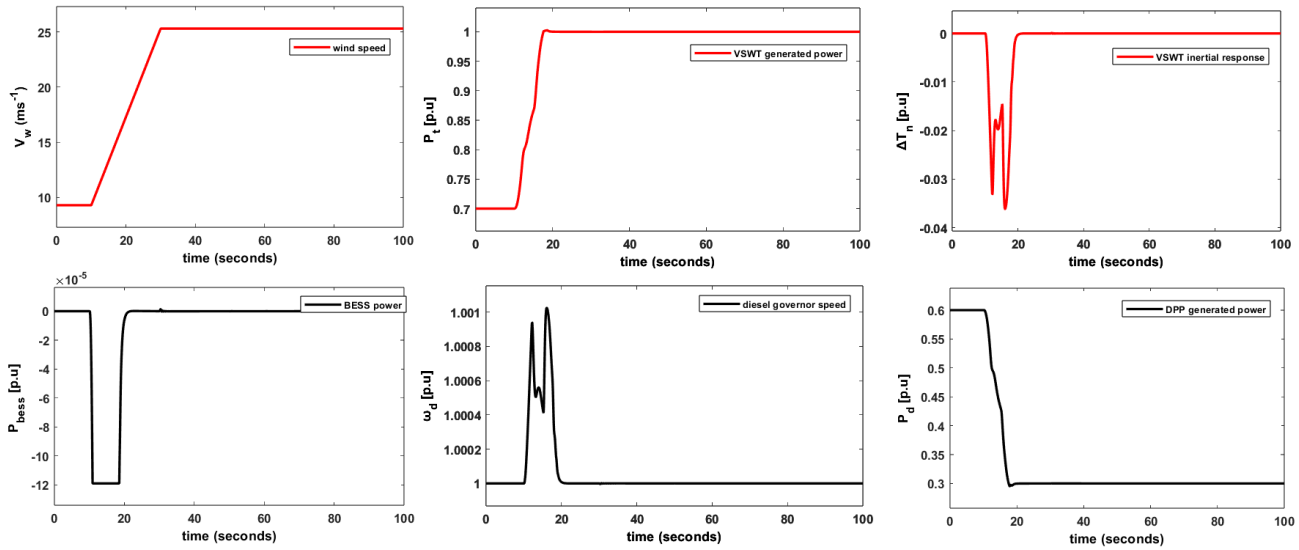

FIGURE 12. Hybrid BESS based WDPS of San Cristobal Island response against gradual increased in wind speed.

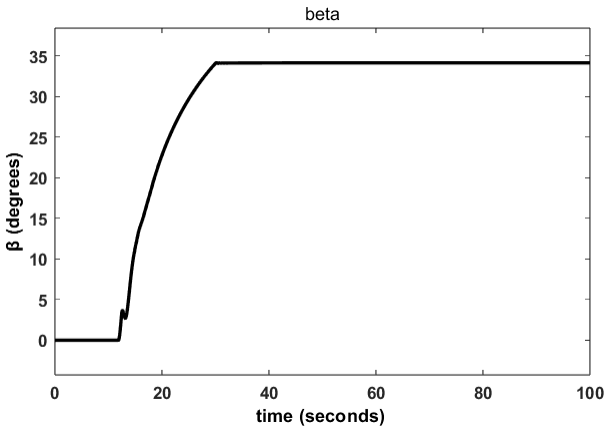

FIGURE 13. BPAC response against steadily increased wind speed (ramp response: Figure 11).

against Case Z several performance parameters of SPBA such as the population size, number of iterations and computational time are 10^{10}, 1279 and 40 minutes approximately, respectively. However, the computational time depends on the speed of CPU of operating system used. In this study the specifications of operating systems used are 1) Processor: AMD Ryzen 9 5950X 16-Core Processor, 3.40GHz 2) Installed RAM: 128 GB.

E. COMPARISON OF SPBA WITH TRADITIONAL TUNING METHODS

In this section, authors compare their proposed tuning methodology with existing traditional tuning methods such as Ziegler-Nichols (ZN), to further validate the results. Before implementing the Ziegler-Nichols, let us briefly describe the basic principle and define the PI formulation according to ZN. According to ZN for tuning a PI controller having gain parameters K_{p_zn} and K_{i_zn}, firstly the integral controller gain is set to zero. Then the value of proportional gain is increased until a stable and continued oscillation response is observed. The gain against which this particular response is observed is referred as ultimate gain, K_u. Similarly, the time-period of such oscillation is termed as ultimate period, P_u. To get the gain parameters, Equations 10 and 11 provide a relationship between K_{p_zn}, K_{i_zn}, K_u and T_u.

$$K_{p\_zn} = 0.45\, K_u \tag{10}$$

$$K_{i\_zn} = 0.54 \frac{K_u}{T_u} \tag{11}$$

It is important to mention that in all cases X, Y and Z, at least two power frequency controllers are tuned simultaneously while a third one remains unchanged. However, ZN tuning methodology is applicable only to a single PI controller at a time. Therefore, ZN cannot provide a global optimized solution while SPBA does. For this reason, to highlight the different performance between these two tuning methodologies, let's start tuning the DPP gain parameters while VSWT will operate at constant V_w. So, to find the ultimate gain parameter and ultimate period of stable oscillation response for DPP, a fixed 0.6 pu load demand is considered. It is observed that $K_u = 110$ and $T_u = 367.346$ ms. Therefore, $K_{p\_zn} = 49.5$ and $K_{i\_zn} = 161.50$ are calculated according to Equations 10 and 11. To evaluate the power system behavior against contingencies, a perturbation of 0.5 step response is considered as increased in P_{load}. The DPP and VSWT response are shown in Figure 8 (b). It clearly shows that the NADIR in this case is 0.9822 p.u. but oscillations or the number of sign changes in frequency derivatives is significantly larger. Moreover, the settling time is significantly larger than the optimal results shown by SPBA.

Tuning of VSWT proposed droop control keeping DPP controller gains unchanged is not possible because the DPP

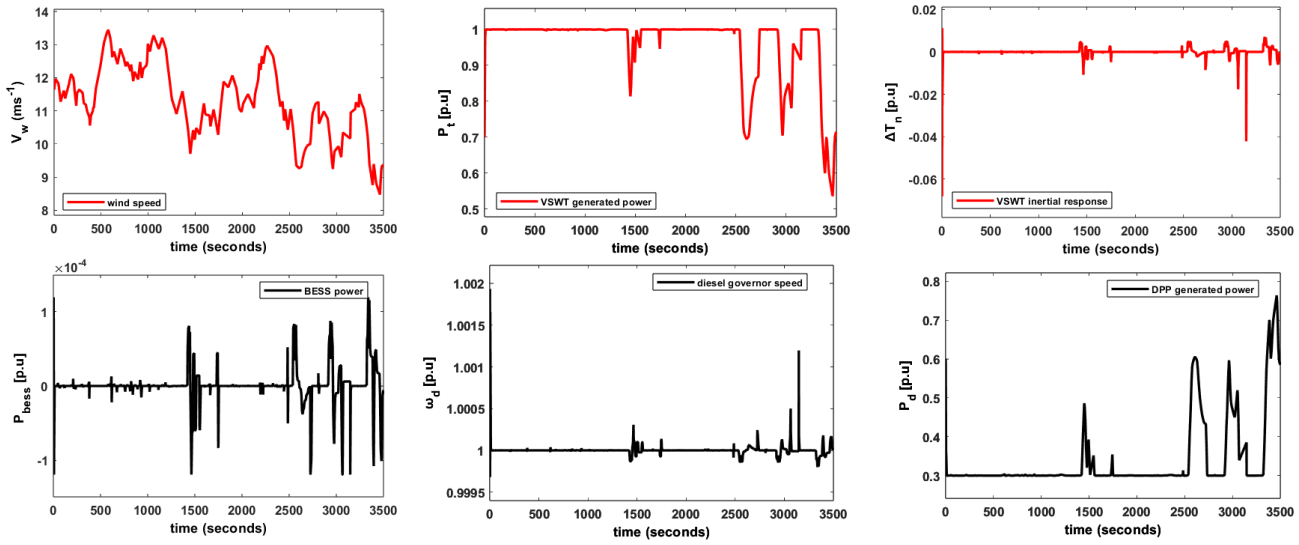

FIGURE 14. Hybrid BESS based WDPS of San Cristobal Island response against random wind speed.

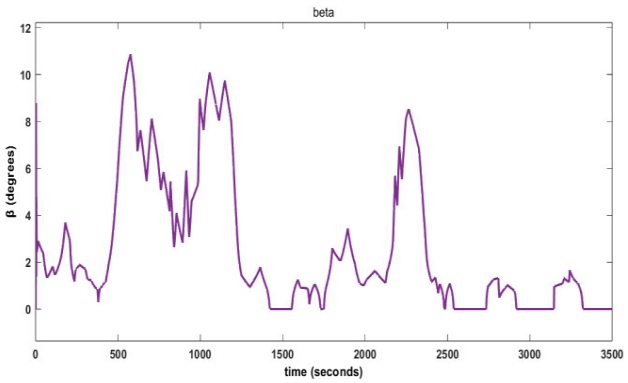

FIGURE 15. BPAC response against random wind speed (Figure 14).

does not allow getting a stable and continuous frequency response changing only the VSWT droop control. The same behavior is observed while tuning BESS gain parameters. Therefore, in comparison with SPBA the following salient features are observed.

1) ZN is not suitable for global optimization while SPBA is.
2) Significant oscillations or number of sign changes in the frequency derivative is observed.
3) ISE and IAE are greater in ZN than SPBA.
4) ZN is not suitable for non-linear and complex systems.

In the above-mentioned discussions, it is mentioned that ZN only tuned DPP in WDPS. Therefore, another option which is offered by MATLAB is the autotuning of PI controllers. So, VSWT proposed proportional controller can be tuned with MALTAB autotuned. However, MATLAB autotuning is unable to tune this control which might happen due to complexity of hybrid power system. Because MATLAB auto tuning first, linearized the system under study, however, in a complex system with multiple objective functions it might not be possible to get results. Another important observation is that MATLAB autotuning doesn't provide global optimum. In other words, no more than one controller of various systems can be tuned simultaneously using MATLAB autotuning. Moreover, the results obtained using MATLAB autotuning might be sub optimal and gain parameters can be adjusted by varying the transient behavior in MATLAB. Therefore, optimized tuning of multi-controllers in a system or multi-system needs new optimization methodology. However, SPBA provide unique global optimized parameters according to Equation 8 because this factor is a compromised solution among several objective functions. Solution at optimum gain parameters reflects reduced NADIR, minimum IAE, minimum ISE and oscillations in frequency derivatives.

VII. SIZING THE BESS

BESS has become more widespread and adopted due to its vast variety of applications, particularly its role in PFC. Nowadays, hybrid RE-based power systems are considerably attracted by BESS due to its ancillary services support, fast response, controllability and geographical independence. However, sizing the battery is a critical task due to environmental challenges (such as dispose of) and economic aspects. In addition, it is a trade-off between technical implications brought by BESS and cost in a particular power system. Moreover, other factors like battery type, degradation factor, cost per kilo watt-hour, energy density, discharge time and optimization etc., make complex selection and sizing of the BESS. However, in this case study, authors focus only on the sizing of the battery in terms of capacity using optimization methodology named SPBA and explore its benefits for San Cristobal Island hybrid WDPS. State of charge (SoC), degradation, life cycle, charging and discharging limits are out of scope of this case study.

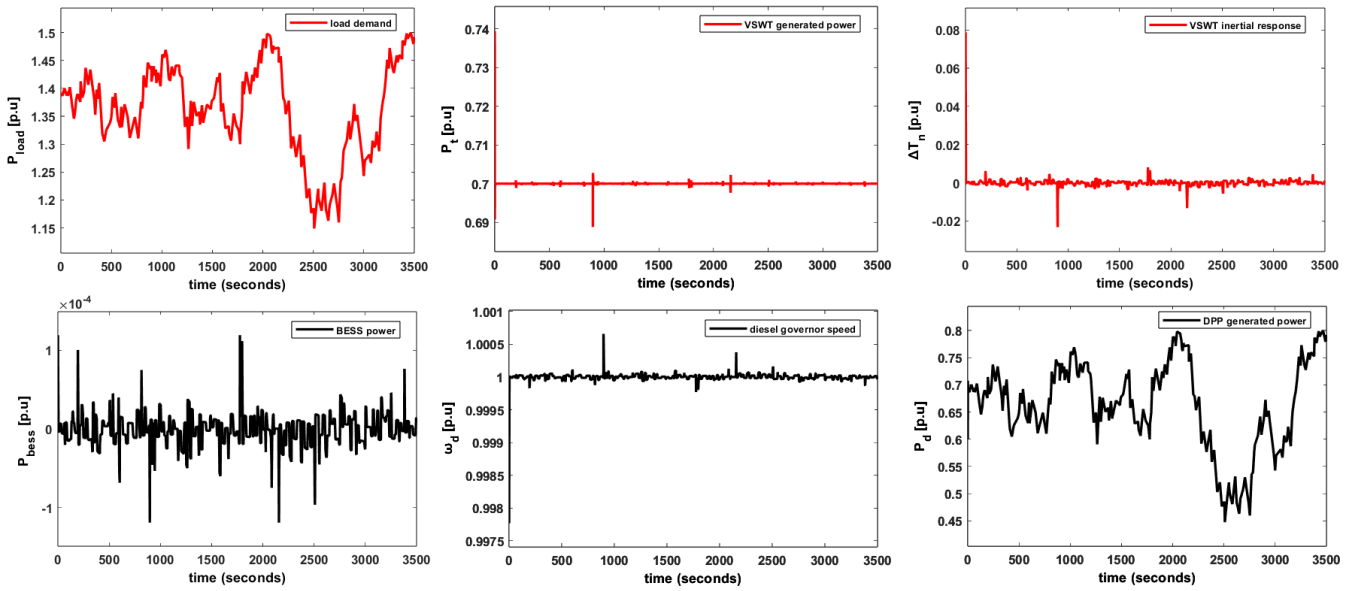

FIGURE 16. Hybrid BESS based WDPS of San Cristobal Island response against random load demand.

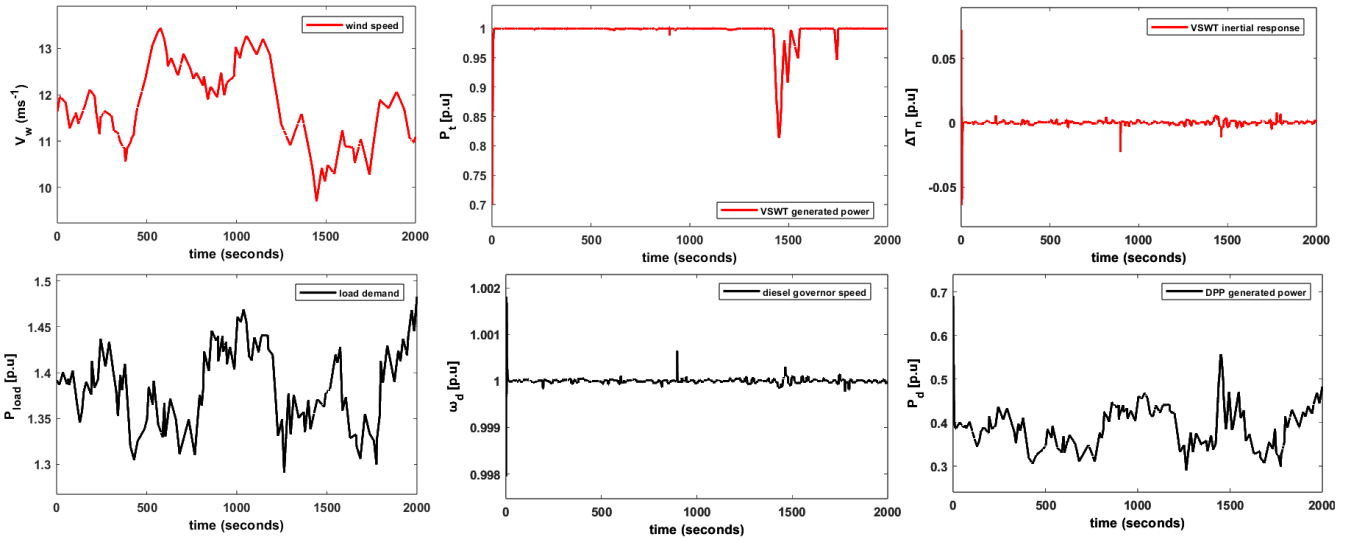

FIGURE 17. Hybrid BESS based WDPS of San Cristobal Island response against simultaneously variation in V_W and load demand.

Using SPBA methodology a step response of 0.5 p.u is considered to optimally tune the gain parameter (K_{bess}) of BESS (Equation (8)) including both DPP and VSWT parameters, simultaneously (discussed in Case Z). Exhaustive search found a unique optimal gain parameter for BESS is 0.6. Against this optimal value, hybrid WDPS have minimum NADIR, lowest IAE, ISE and Z (given in Table 2). Furthermore, this study extends to find the WDPS stability limits. It means that against how much power variation or contingencies, this hybrid WDPS in the presence of BESS, can be operationally stable without operating frequency relay. However, with the integration of BESS hybrid WDPS performed up to $\Delta P_{load} = 1$ p.u in total of contingencies. Nonetheless, the maximum limits of energy released by BESS depend on proposed power system model and its operation. For example, in Figure 10, the VSWT operates at a constant wind speed of 9.2966 ms^{-1} to generate power of 0.7 p.u and initial P_{load} is 1 p.u. It means DPP is responsible to provide the power difference (P_{load}-P_t) i.e., 0.3 p.u. So, the maximum perturbation of 0.7 p.u can be applied to this system at t = 10 sec. In this way the DPP operates at its maximum capacity of 1p.u. Similarly, if the VSWT operates at 0.7 p.u and P_{load} is 0.9 p.u a maximum step of 0.8 p.u as a load increment can be applied to the hybrid system. So, it means initially DPP operates at 0.2 p.u but to fulfill load demand it is responsible to provide 1 p.u (0.2 p.u initial power +

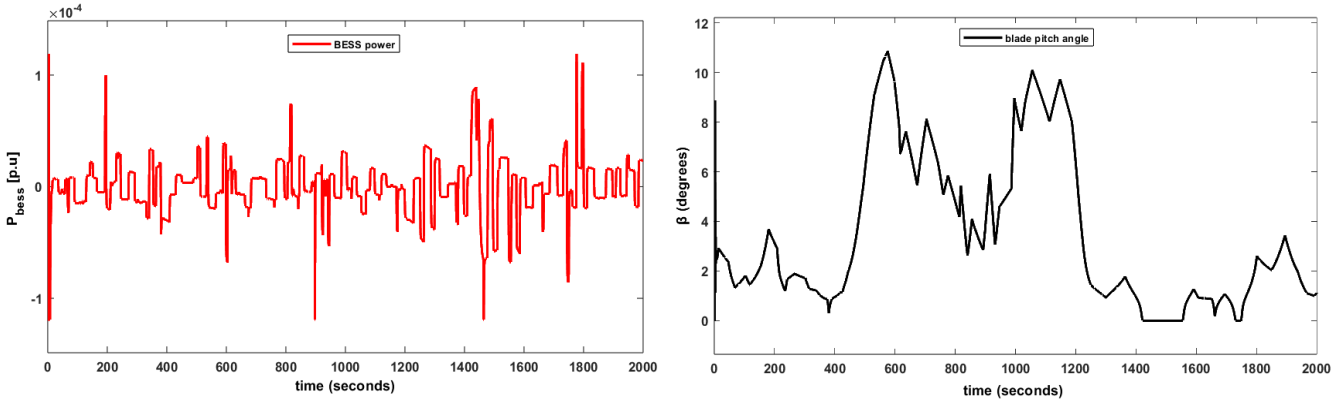

FIGURE 18. BESS and BPAC response against simultaneous variation in V_w and load demand (Figure 17).

0.8 p.u. load increment). It is concluded that DPP is always responsible to provide the power imbalance between supply and demand.

Furthermore, it clearly shows that BESS sizing solely depends on the nature of the power system in which it is installed. In addition, the DPP initial stage is also one of the factors in the sizing of BESS. In a real-world scenario, DPP is not shut down, DPP must be operated at least at some minimal level to provide energy. In addition, other constraints, such as torque or rotor speed limits, VSWT limits, BPAC limits, and BESS storage charging or discharging limits or BESS time constant etc., play a vital role in the sizing of BESS. It is important to mention that the BESS role in this research is only to facilitate PFC purposes. Therefore, in this case study, authors choose BESS sizing according to following criteria. First the VSWT operates at its full load, i.e., 1 p.u, to get more advantage of available clean energy. Second DPP operates at least 30% of full load (low load condition) to allow maximum penetration of renewable energy in diesel fuel. It means that the BESS must be designed with 0.7 p.u (450kW) of perturbation (0.7 p.u = 2 p.u (max. power) – 1 pu (max. P_t) – 0.3 p.u (min. P_d)). It is clear in Figure 11, with perturbation of 0.7 p.u. step response, the BESS will release 9.119×10^{-3}p.u power (P_{bess}) i.e., 5.92735 kW and 4.5435 kJ. So, the P_{bess} defines the BESS sizing to assist PFC in hybrid WDPS of San Cristobal Island.

VIII. HYBRID WDPS AND PROPOSED CONTROL PERFORMANCE UNDER REAL WORLD SCENARIOS

In this section, authors further consider various sets of perturbations such as step, ramp and random as realistic events in this study, to justify the performance of a hybrid WDPS, the proposed control and its tuning. Because in literature [48], these perturbations are considered as sufficient parameters to justify the performance of a controller. Therefore, step, ramp and random perturbations represent the sudden increase in load demand or loss of wind generator, wind speed steadily increases and load demand and /or V_w, respectively. Therefore, after exhaustive research shown in Section VI, Case Z

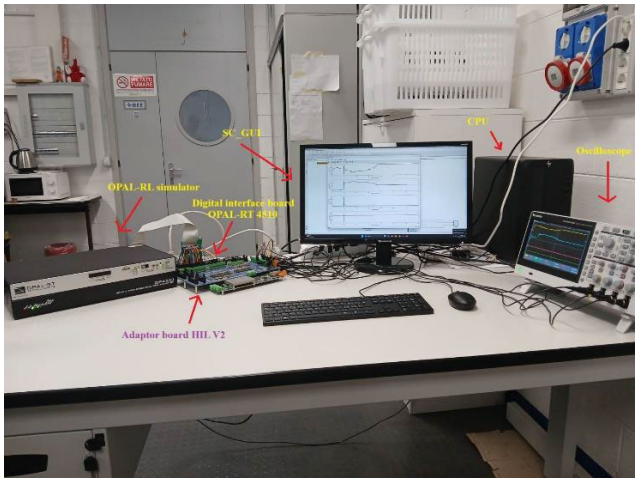

FIGURE 19. OPAL-RT setup at Department of Electrical, Computer and Biomedical Engineering, University of Pavia, Italy.

is considered for further study due to its better performance against FD. So, for step response (sudden P_{load} increased or loss of wind generator), Case Z itself is an example. However, Figure 12 shows the behavior of WDPS against a steady increase in wind speed ($\Delta V_w \approx 0.81$ ms^{-2}). However, P_{load} is fixed at 1.1 p.u and DPP only provides the difference in the power demand. Slight variation (0.001 p.u) in diesel governor rotor speed is due to the variation in the MPPT of VSWT. When VSWT speed moves from one MPPT region to another then this behavior is observed but it lasts just a few seconds. It is important to mention that this hybrid BESS model can perform stable beyond this steady increase in wind speed until the BPAC allowable limit (2°/sec) supersede and cut-in wind speed i.e., 25 ms^{-1} [49] in this case. So, Figure 13 shows the BPAC response against this ramp response, which clearly shows its smooth rotation.

Finally, WDPS and controller performance are tested against random response. The authors classified random response into three different scenarios: (1) random variation in wind speed while load demand is constant (2) wind

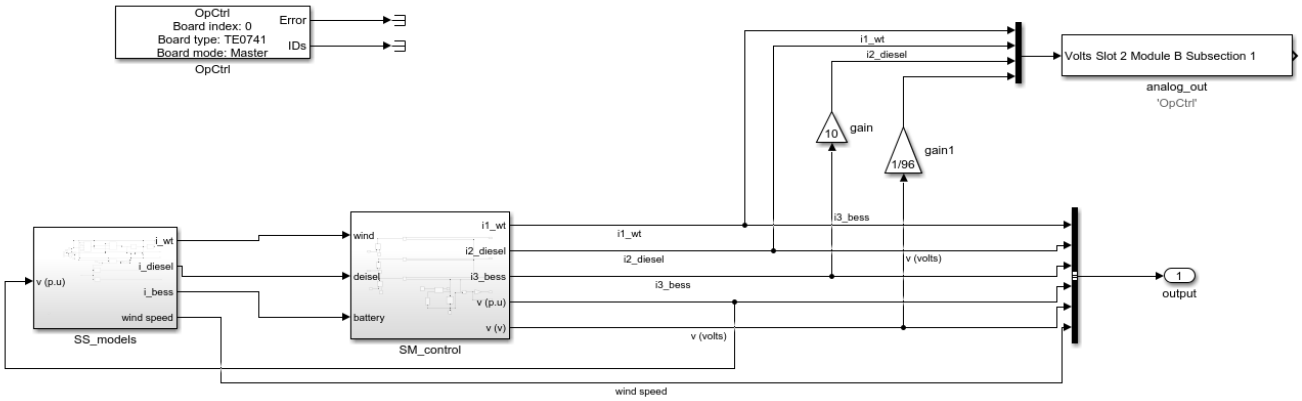

FIGURE 20. OPAL-RT block representation of hybrid BESS based WDPS.

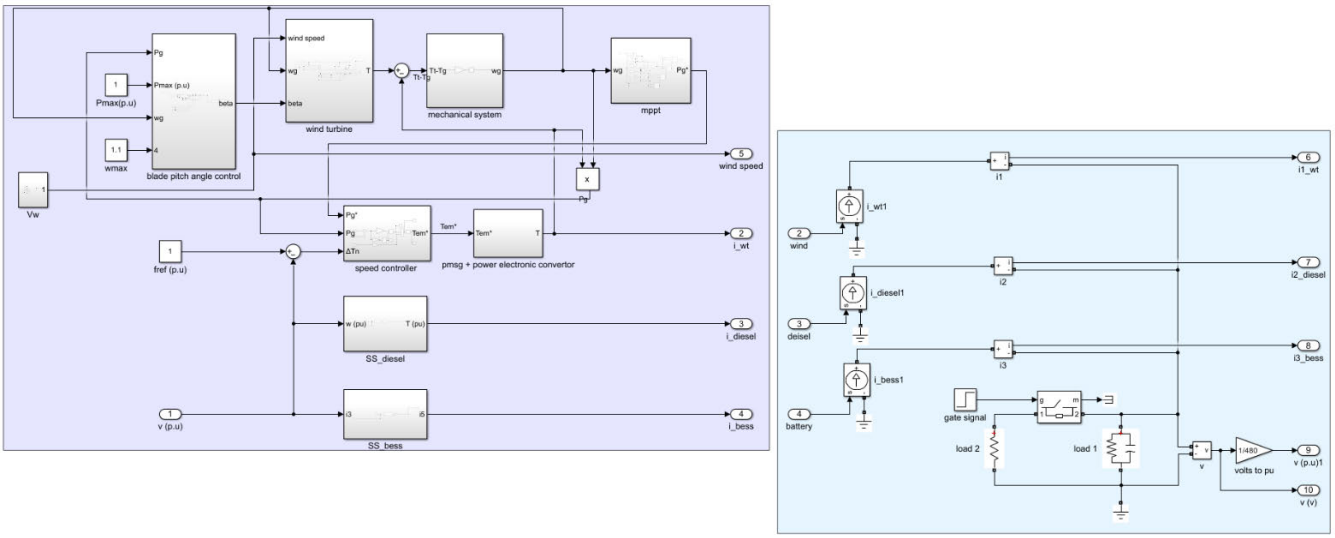

FIGURE 21. Detailed schematic of Figure 18 blocks: SS_models (left side) and SM_control (right side).

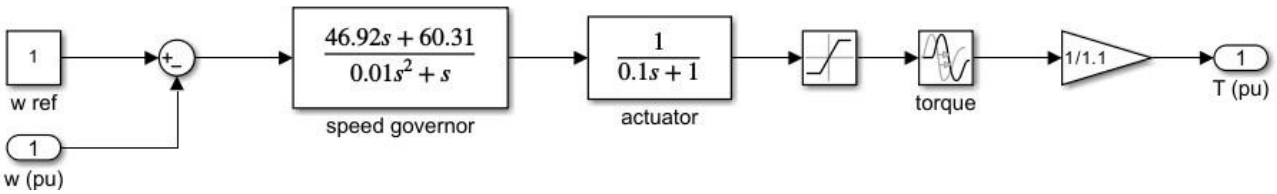

FIGURE 22. Detailed diesel governor representation for LFC studies.

speed is constant while load demand randomly increases or decreases and (3) both wind speed and load demand vary simultaneously. In this way, almost all major possibilities of real-world scenarios for hybrid WDPS can be studied. However, although many other events can happen, the above scenarios can be considered enough to show the behavior of BESS, VSWT and DPP during contingencies. So, Figure 14 shows the hybrid WDPS response against variable wind speed while P_{load} is constant (1.3 p.u). It clearly shows that BPAC adjusts the blade rotation (Figure 15) to avoid any damage, particularly when VSWT exceeds 1 p.u. DPP produced only the difference between P_{load} and P_t, that's why it maintains the value of 0.3 p.u. In addition, the diesel rotor speed is almost 1 p.u which shows its governor effectiveness. BESS and synthetic control effectiveness clearly reflect in Figure 14. Similarly, Figure 16 shows the behavior of hybrid WDPS in case of variable load demand while wind speed is constant (9.2966 ms^{-1}). Moreover, Figures 17 and 18 show

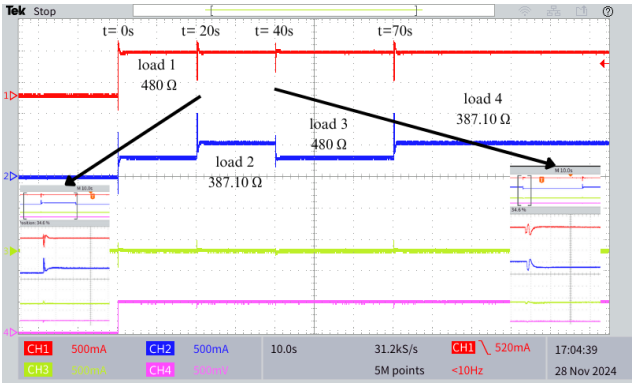

FIGURE 23. Real time current and voltage measurements of various power systems during load variation.

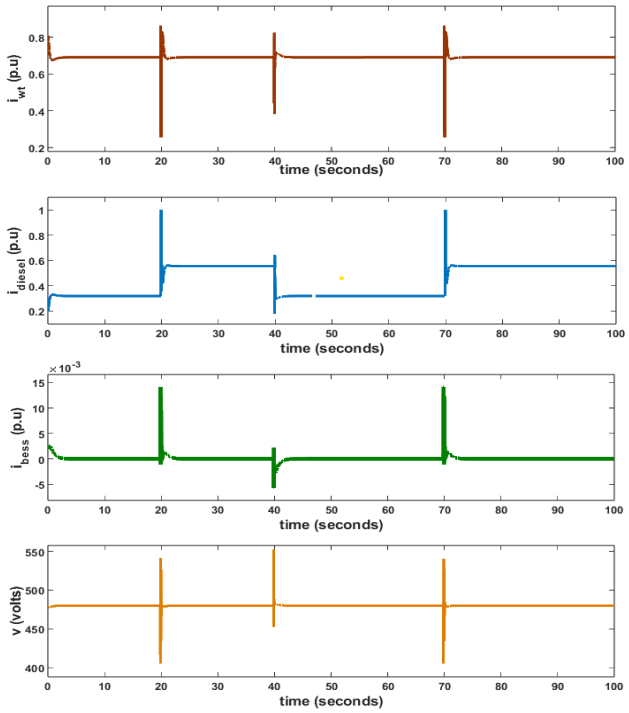

FIGURE 24. SC_GUI scope current and voltage measurements of various power systems during load variation.

the power system's effectiveness during simultaneous change in load demand and wind speed. All the above-mentioned difference scenarios represent real-world contingencies.

IX. HYBRID BESS BASED WDPS EMULATION ON OPAL-RT

OPAL-RT is a Linux based real-time high-speed simulator that allows MATLAB Simulink models to interact with real world in real time [50]. Therefore, the hybrid BESS discussed above is emulated in an OPAL-RT environment. For this purpose, RT-LAB, a real-time software, is used to configure the MATLAB Simulink model according to the OPAL-RT criteria i.e., differentiate computational subsystems (SM_computation, SS_computation: subsystems used for all type of calculations etc.) and GUI subsystems (SC_GUI (graphic user interface): subsystems have only constants, inputs, outputs etc.) and assign these subsystems to various cores of OPAL-RT [51], [52]. Finally, maximizing parallel execution and running offline ensures model performance under study. It is important to mention that the data between various computational subsystems are synchronously transferred while it is asynchronously transferred between computational and GUI subsystems [51]. Moreover, the offline model undergoes three further processes (i.e., build, load and execute) to be run in real time.

In this paper, hardware in the loop (HIL) is developed to test the hybrid BESS based WDPS in real time, shown in Figure 19 and 20. It clearly shows in Figure 21 that SS_model have all three power systems (wind, diesel and battery) but SM_control represents the three parallel connected current source with resistive load. In this way, hybrid BESS based WDPS is emulated as a current and voltage balanced model for LFC studies. However, the schematic of diesel governor is shown in Figure 22. It is important to mention that the inertial constant is reflected as an equivalent capacitance in parallel with the load. In this topology, the voltage remains constant, but the current varies with load variation. It means that torque and frequency in section VI and VIII are emulated as current and voltage, respectively. Therefore, the torque produced by various subsystems (Figure 21) is used as a current input (I) for controlling current sources. And voltage variation across the loads is used as input to diesel governor, droop control in wind turbine and BESS control. During normal operations the voltage remains constant, and all three subsystems operate smoothly. However, during contingencies such as wind or load fluctuation the voltage varied for its nominal value and all three subsystems provide PFC. WDPS and BESS provide inertial support by varying the current (i.e., torque) while DPP is responsible to match load demand, in addition to inertial support. It is important to mention that the power provided by DPP is in terms of current increase or decrease because voltage remains constant. Similarly, the wind power plant provides current either constant or variable according to wind speed. However, it provides inertial support during transients (i.e., loss of generator etc.). Consequently, BESS release or absorb current whenever needed and restore the voltage to its nominal value. Below mentioned are several tests in a real-time environment that show the effectiveness of this study.

A. HYBRID BESS RESPONSE AGAINST LOAD VARIATION

In this case, hybrid BESS based WDPS undergoes load variation at various time intervals while wind speed (V_w) is constant i.e., 9.2866 ms^{-1}. Figure 23 shows the real time measurements in OPAL-RT environment on oscilloscope while Figure 24 shows the hybrid power system performance at SC_GUI (or desktop scope display). In Figure 23, one box along x-axis on oscilloscope is equal to 10sec, while one box along y-axis is equal to 0.5 mA (milliampere) or 0.5mV

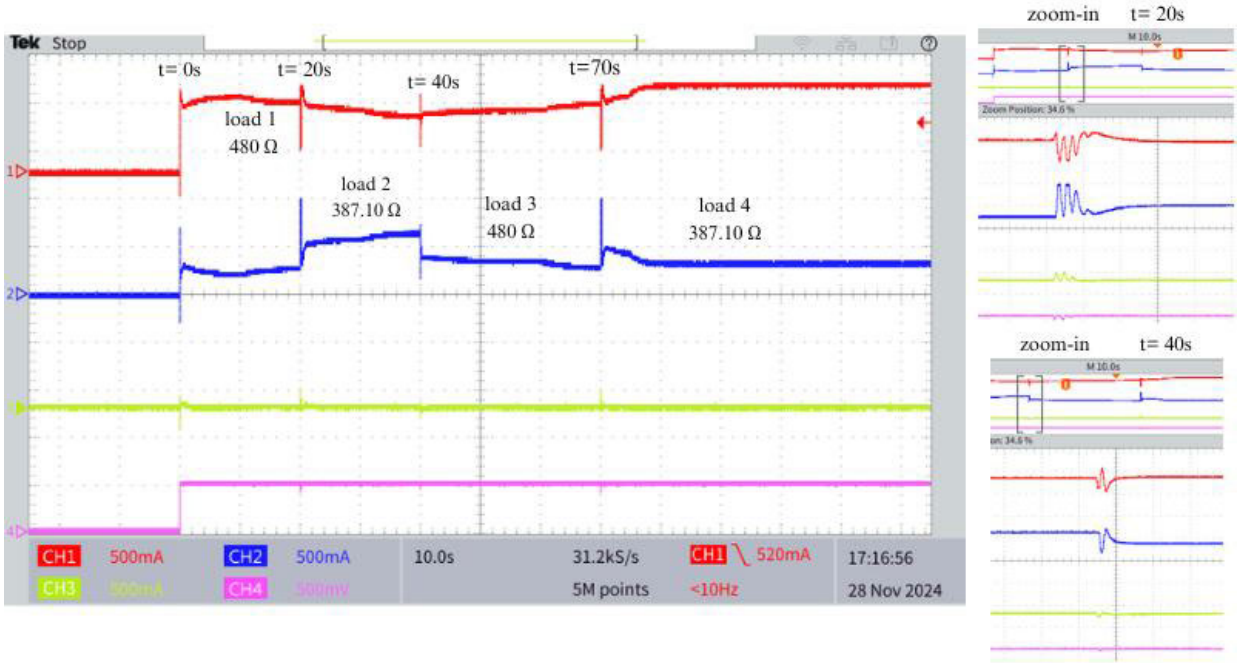

FIGURE 25. Real time current and voltage measurements of various power systems during simultaneously changed in load and wind speed.

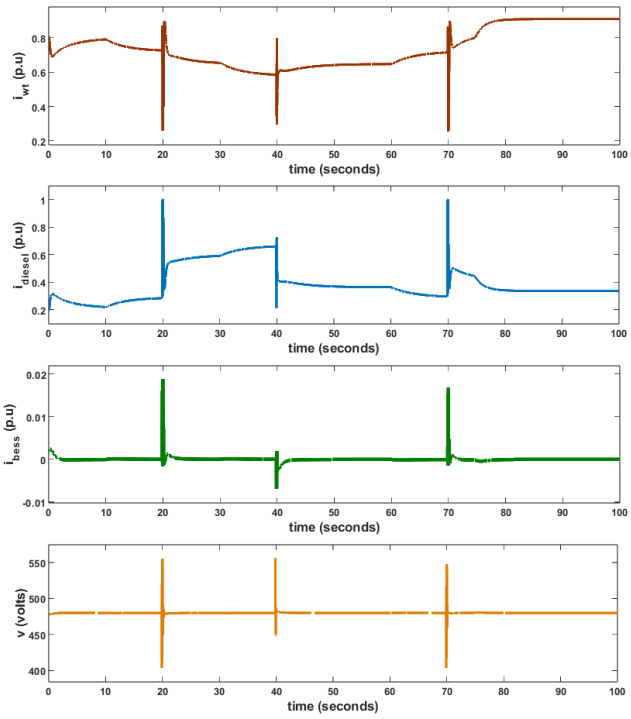

FIGURE 26. SC_GUI scope current and voltage measurements of various power systems during simultaneously changed in load and wind speed.

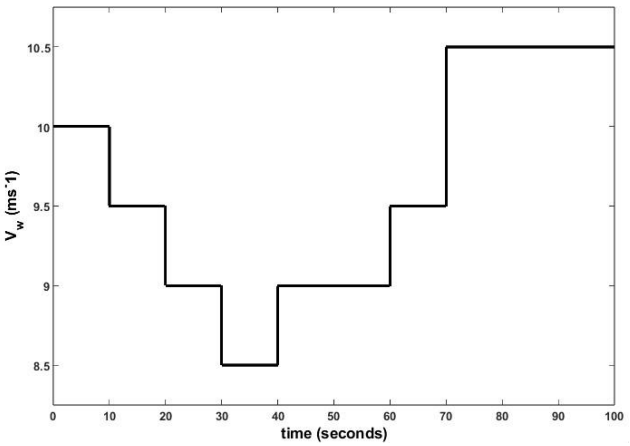

FIGURE 27. Variable wind speed.

(millivolts). It means the total time-period along x-axis is 150sec while total mA or mV along y-axis equal to total 5mA or 5mV, respectively. It clearly shows that the wind power plant (CH1 — oscilloscope channel 1) generates constant current while contributing to providing inertial support, against load variation (or voltage fluctuations). Similarly, the diesel power plant (CH2) fulfilled the load demand. However, BESS (CH3) also provides inertial support by absorbing or supplying current against such load variation. However, the voltage behavior (CH4) seems to be constant against load variation. Distribution of load at various time intervals are t = 0 to 20 sec load demand is constant at 480 ohms, between time intervals 20 sec to 40 sec load demand is 387.10 ohms (decreased by 98.9 ohms), between time intervals t = 40 sec to 70 sec load demand is 400 ohms (increased by 12.90 ohms). Finally, load demand is maintained at 387.10 ohms between time intervals 70 sec to onwards (decreased by 12.90 ohms).

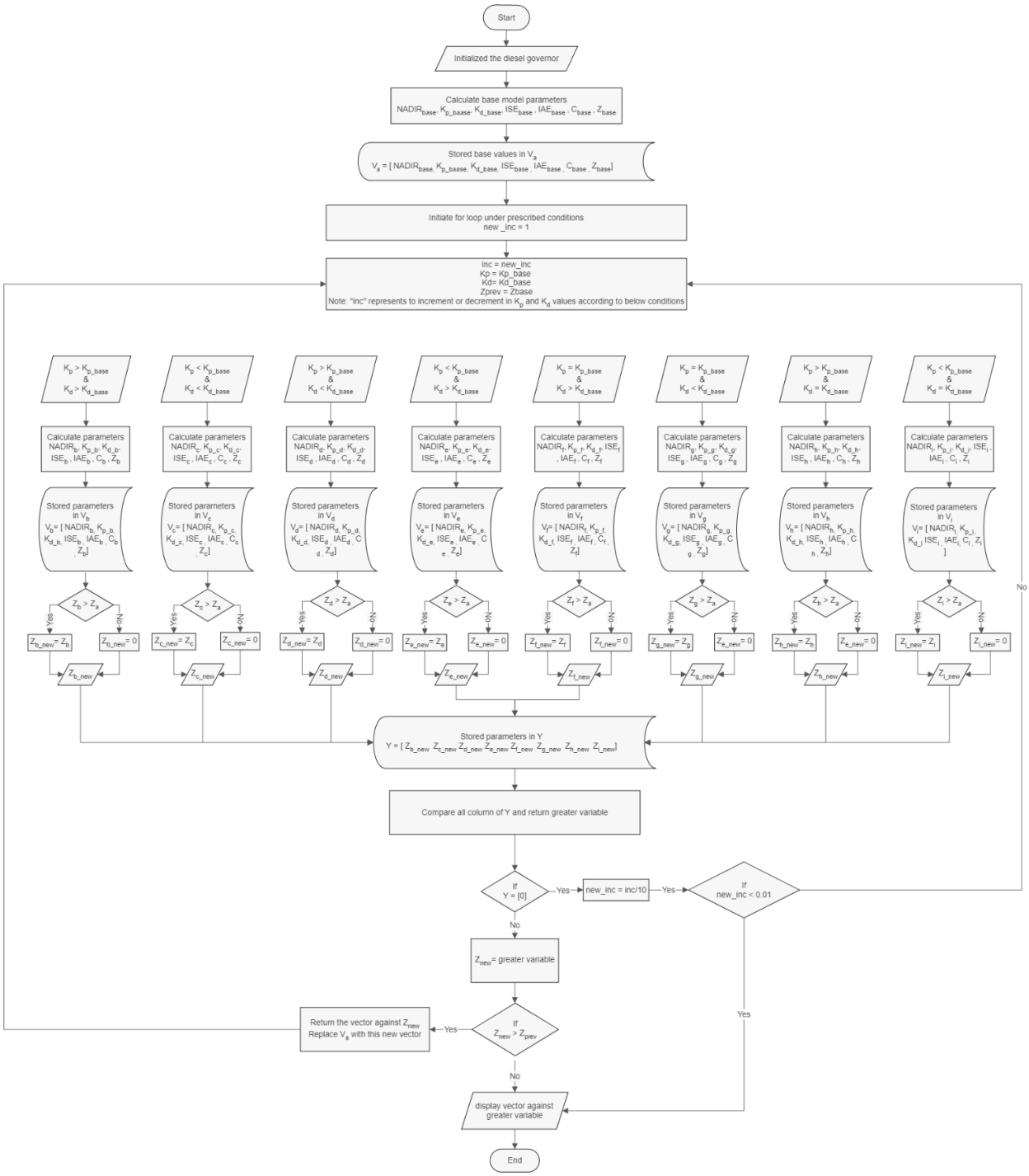

FIGURE 28. Student psychology based algorithm methodology flow chart for a PI controller.

B. BESS WDPS RESPONSE AGAINST SIMULTANEOUS CHANGES IN WIND SPEED AND LOAD DEMAND

In this case, hybrid BESS based WDPS undergoes simultaneously wind fluctuations and variable load. Figures 25 and 26 clearly show the behavior of the hybrid power system. It shows that the current produced by wind turbine is variable, according to the available V_w (Figure 27), while diesel power plant managed its production according to required load demand. It is important to mention that the distribution of load is the same as mentioned in the previous section IX-A. At t = 0 to 20 sec load demand is constant at 480 ohms, but wind speed varied. Therefore, the diesel power plant fulfilled the required load demand while the wind turbine produced current according to available wind speed. Between time intervals 20 sec to 40 sec load demand is decreased by 98.9 ohms and wind also varied. So, wind turbines and

TABLE 3. Dataset of DPS installed at San-Cristobal Island [39].

Symbol	Parameters	Values
	Model of diesel engine	CAT-3512 DITA
f	Frequency	60 Hz
S	Capacity	813 KVA
t_1/ t_2/ t_3	Time constants	0.024 s/ 0.1 s/ 0.01 s
T_{max}/ T_{min}	Torque max/ min	1.1 p.u/ 0 p.u
V_{out}	Output voltage	480 V ± 5%
P_{rated}	Rated power	650 kW
H_T	Constant of inertia	0.4208 s
N_s	Synchronous speed	1200 RPM

TABLE 4. San-Cristobal Island WT parameters [20].

Symbols	Parameters	Values
P_{base}	Base power	800kW
P_g	Generator power min/ max	0.04p.u/ 1 p.u
f_{nom}	Nominal frequency of generator	50Hz
K_{opt}	Optimization constant	0.6728
K_{ppc}/K_{ipc}	Blade pitch controller gains parameters	1300/ 150
D	Diameter of VSWT rotor	59m
K_{pc}/ K_{ic}	Pitch compensation controller parameters	0/ 150
$d\beta/dt$, $_{min/max}$	Rate of pitch angle min/ max	-2^0/s / $+2^0$/s
$V_{w,\,nom}$	Nominal wind speed	10ms^{-1}
H_i	Constant of inertia	4.18
K_{ppc} /K_{ipc}	Gains of PI pitch controller	150/ 25
$T_{em,\,min/max}$	Electromagnetic torque min/ max	0.08p.u/ 0.91 p.u
n_1, n_2, n_3, n_4, n_5, n_6	Constants of MPPT curve	0.5176, 116, 0.4, 5, 21, 0.0068
ω_{min}, ω_0, ω_1, ω_{max}	Speed limits of MPPT	0.5p.u, 0.51p.u, 1.09p.u, 1.1p.u.
τ_c	Time constant of generator and electronics convertor	20ms
P	Air density	1.225kgm^{-3}
τ_p	Servo-motor time constant	0.3s
K_{psc}/ K_{isc}	Gain parameters of speed controller min/max	0.3/ 8
$\omega_{t,\,base}$	Turbine base speed	2.3 rad/s
$\omega_{g,\,base}$	Base speed of generator	157.08 rad/s

diesel power plants contribute to providing inertial support at 20 sec but diesel power plant is also responsible to provide the difference of current demand. Similarly, between time intervals t = 40 sec to 70 sec load demand is increased by 12.90 ohms and finally, load is decreased by 12.90 ohms at t = 70 sec to maintain its constant value 387.10 ohms. However, wind turbine production is limited due to the wind speed.

Real time simulation in OPAL-RT environment justifies the performance of hybrid BESS based WDPS of San Cristobal Island.

X. CONCLUSION

Frequency excursions is one of the major problems of isolated hybrid RE power system during contingencies. One of the reasons is the intermittent nature of RE resource availability. In this paper, a BESS is proposed for San Cristobal Island hybrid WDPS to provide PFC. Naturally, VSWT provide negligible inertial support due to fast acting power converters, during contingencies. Therefore, a synthetic (droop) control in VSWT is introduced in VSWT which helps the VSWT to release inertia. Proposed controllers in hybrid BESS based WDPS are tuned with SPBA because it provides unique optimal solution with reduced NADIR, IAE, ISE and number of sign changes in frequency derivatives. If gain parameters increased or decreased from optimal gain values then results will be worse in terms of enhanced NADIR, settling time and oscillations. Furthermore, hybrid BESS based WDPS are tuned and compared by considering various scenarios such as: VSWT and BESS while DPP parameters remain unchanged (Case X), DPP and BESS while VSWT parameters unchanged (Case Y), and last, DPP, VSWT and BESS tuned as a whole (Z). Results show that Case Z is more effective than the rest of the scenarios. FD is improved by 0.3 Hz as compared to base case against a contingency of 0.5 p.u step (increase in load demand). In addition, a BESS size of 5.92735 kW (i.e., 0.9119 % of DPP rated power) and 4.5435 kJ is proposed in this research. Moreover, the hybrid BESS based WDPS is tested under various set of perturbations i.e., loss of wind generator, steady increase in wind speed ($\Delta V_w \approx 0.81$ ms^{-2}), variable wind speed, variable load demand and simultaneous change in V_w and P_{load}. Finally, the emulation of hybrid BESS based WDPS is tested in real time to validate its performance. Simulation results against all these perturbations show the effectiveness and impact of BESS on hybrid WDPS of San Cristobal Island.

APPENDIX

See Tables 3 and 4, and Figure 28.

REFERENCES

[1] M. A. Bagherian and K. Mehranzamir, "A comprehensive review on renewable energy integration for combined heat and power production," *Energy Convers. Manage.*, vol. 224, Nov. 2020, Art. no. 113454, doi: 10.1016/j.enconman.2020.113454.

[2] A. Q. Al-Shetwi, "Sustainable development of renewable energy integrated power sector: Trends, environmental impacts, and recent challenges," *Sci. Total Environ.*, vol. 822, May 2022, Art. no. 153645, doi: 10.1016/j.scitotenv.2022.153645.

[3] M. Ranjan and R. Shankar, "A literature survey on load frequency control considering renewable energy integration in power system: Recent trends and future prospects," *J. Energy Storage*, vol. 45, Jan. 2022, Art. no. 103717, doi: 10.1016/j.est.2021.103717.

[4] S. Impram, S. Varbak Nese, and B. Oral, "Challenges of renewable energy penetration on power system flexibility: A survey," *Energy Strategy Rev.*, vol. 31, Sep. 2020, Art. no. 100539, doi: 10.1016/j.esr.2020.100539.

[5] D. Nikolic and M. Negnevitsky, "Practical solution for the low inertia problem in high renewable penetration isolated power systems," in *Proc. IEEE Power Energy Soc. Gen. Meeting (PESGM)*, Aug. 2018, pp. 1–5, doi: 10.1109/PESGM.2018.8586001.

[6] M. Asad and J. Á. Sánchez-Fernández, "Frequency regulation provided by doubly fed induction generator based variable-speed wind turbines using inertial emulation and droop control in hybrid wind–diesel power systems," *Appl. Sci.*, vol. 15, no. 10, p. 5633, May 2025, doi: 10.3390/app15105633.

[7] D. M. Greenwood, K. Y. Lim, C. Patsios, P. F. Lyons, Y. S. Lim, and P. C. Taylor, "Frequency response services designed for energy storage," *Appl. Energy*, vol. 203, pp. 115–127, Oct. 2017, doi: 10.1016/j.apenergy.2017.06.046.

[8] L. Sigrist, L. Rouco, and F. M. Echavarren, "A review of the state of the art of UFLS schemes for isolated power systems," *Int. J. Electr. Power Energy Syst.*, vol. 99, pp. 525–539, Jul. 2018, doi: 10.1016/j.ijepes.2018.01.052.

[9] P. Tielens and D. Van Hertem, "The relevance of inertia in power systems," *Renew. Sustain. Energy Rev.*, vol. 55, pp. 999–1009, Mar. 2016, doi: 10.1016/j.rser.2015.11.016.

[10] I. Egido, L. Sigrist, E. Lobato, L. Rouco, and A. Barrado, "An ultracapacitor for frequency stability enhancement in small-isolated power systems: Models, simulation and field tests," *Appl. Energy*, vol. 137, pp. 670–676, Jan. 2015, doi: 10.1016/j.apenergy.2014.08.041.

[11] H. Bevrani, *Robust Power System Frequency Control*, 2nd ed., Cham, Switzerland: Springer, 2014, doi: 10.1007/978-3-319-07278-4.

[12] M. N. H. Shazon, N.-Al-Masood, H. M. Ahmed, S. R. Deeba, and E. Hossain, "Exploring the utilization of energy storage systems for frequency response adequacy of a low inertia power grid," *IEEE Access*, vol. 9, pp. 129933–129950, 2021, doi: 10.1109/ACCESS.2021.3114216.

[13] A. Fernández-Guillamón, E. Gómez-Lázaro, E. Muljadi, and Á. Molina-García, "Power systems with high renewable energy sources: A review of inertia and frequency control strategies over time," *Renew. Sustain. Energy Rev.*, vol. 115, Nov. 2019, Art. no. 109369, doi: 10.1016/j.rser.2019.109369.

[14] R. Rajan, F. M. Fernandez, and Y. Yang, "Primary frequency control techniques for large-scale PV-integrated power systems: A review," *Renew. Sustain. Energy Rev.*, vol. 144, Jul. 2021, Art. no. 110998, doi: 10.1016/j.rser.2021.110998.

[15] W. Ji, F. Hong, Y. Zhao, L. Liang, H. Du, J. Hao, F. Fang, and J. Liu, "Applications of flywheel energy storage system on load frequency regulation combined with various power generations: A review," *Renew. Energy*, vol. 223, Mar. 2024, Art. no. 119975, doi: 10.1016/j.renene.2024.119975.

[16] D. Ochoa and S. Martinez, "Proposals for enhancing frequency control in weak and isolated power systems: Application to the wind-diesel power system of San Cristobal Island–Ecuador," *Energies*, vol. 11, no. 4, p. 910, Apr. 2018, doi: 10.3390/en11040910.

[17] M. Martín-Betancor, J. Osorio, A. Ruíz-García, and I. Nuez, "Technical-economic limitations of floating offshore wind energy generation in small isolated island power systems without energy storage: Case study in the Canary Islands," *Energy Policy*, vol. 188, May 2024, Art. no. 114056, doi: 10.1016/j.enpol.2024.114056.

[18] N. Skopetou, P. A. Zestanakis, R. Rotas, P. Iliadis, C. Papadopoulos, N. Nikolopoulos, A. Sfakianakis, and C. Koroneos, "Energy analysis and environmental impact assessment for self-sufficient non-interconnected islands: The case of nisyros island," *J. Cleaner Prod.*, vol. 447, Apr. 2024, Art. no. 141647, doi: 10.1016/j.jclepro.2024.141647.

[19] J. Van de Vyver, J. D. M. De Kooning, B. Meersman, L. Vandevelde, and T. L. Vandoorn, "Droop control as an alternative inertial response strategy for the synthetic inertia on wind turbines," *IEEE Trans. Power Syst.*, vol. 31, no. 2, pp. 1129–1138, Mar. 2016, doi: 10.1109/TPWRS.2015.2417758.

[20] M. Asad and J. A. Sanchez-Fernandez, "Enhancing frequency regulation support through several synthetic inertial approaches for WDPS," *Electronics*, vol. 13, no. 5, p. 852, Feb. 2024, doi: 10.3390/electronics13050852.

[21] G. Martínez-Lucas, J. Sarasua, and J. Sánchez-Fernández, "Frequency regulation of a hybrid wind–hydro power plant in an isolated power system," *Energies*, vol. 11, no. 1, p. 239, Jan. 2018, doi: 10.3390/en11010239.

[22] O. R. Llerena-Pizarro, R. P. Micena, C. E. Tuna, and J. L. Silveira, "Electricity sector in the galapagos islands: Current status, renewable sources, and hybrid power generation system proposal," *Renew. Sustain. Energy Rev.*, vol. 108, pp. 65–75, Jul. 2019, doi: 10.1016/j.rser.2019.03.043.

[23] J. Ayala-Pico, D. Arcos–Aviles, A. Ibarra, C. Fernandez, F. Guinjoan, and W. Martinez, "Current development of electricity generation systems in the Galapagos Islands–Ecuador," *Renew. Energy Focus*, vol. 46, pp. 88–102, Sep. 2023, doi: 10.1016/j.ref.2023.06.003.

[24] M. A. Ponce-Jara, M. Castro, M. R. Pelaez-Samaniego, J. L. Espinoza-Abad, and E. Ruiz, "Electricity sector in ecuador: An overview of the 2007–2017 decade," *Energy Policy*, vol. 113, pp. 513–522, Feb. 2018, doi: 10.1016/j.enpol.2017.11.036.

[25] M. H. El-Bahay, M. E. Lotfy, and M. A. El-Hameed, "Computational methods to mitigate the effect of high penetration of renewable energy sources on power system frequency regulation: A comprehensive review," *Arch. Comput. Methods Eng.*, vol. 30, no. 1, pp. 703–726, Jan. 2023, doi: 10.1007/s11831-022-09813-9.

[26] M. R. Amin, M. Negnevitsky, E. Franklin, K. S. Alam, and S. B. Naderi, "Application of battery energy storage systems for primary frequency control in power systems with high renewable energy penetration," *Energies*, vol. 14, no. 5, p. 1379, Mar. 2021, doi: 10.3390/en14051379.

[27] F. Arrigo, E. Bompard, M. Merlo, and F. Milano, "Assessment of primary frequency control through battery energy storage systems," *Int. J. Electr. Power Energy Syst.*, vol. 115, Feb. 2020, Art. no. 105428, doi: 10.1016/j.ijepes.2019.105428.

[28] G. L. Kyriakopoulos and G. Arabatzis, "Electrical energy storage systems in electricity generation: Energy policies, innovative technologies, and regulatory regimes," *Renew. Sustain. Energy Rev.*, vol. 56, pp. 1044–1067, Apr. 2016, doi: 10.1016/j.rser.2015.12.046.

[29] G. Rancilio, A. Rossi, D. Falabretti, A. Galliani, and M. Merlo, "Ancillary services markets in europe: Evolution and regulatory trade-offs," *Renew. Sustain. Energy Rev.*, vol. 154, Feb. 2022, Art. no. 111850, doi: 10.1016/j.rser.2021.111850.

[30] A. Eydeland and W. Krzysztof, *Energy and Power Risk Management: New Developments in Modeling, Pricing, and Hedging*. Hoboken, NJ, USA: Wiley, 2002.

[31] Y. Hu, M. Armada, and M. J. Sánchez, "Potential utilization of battery energy storage systems (BESS) in the major European electricity markets," *Appl. Energy*, vol. 322, Sep. 2022, Art. no. 119512, doi: 10.1016/j.apenergy.2022.119512.

[32] A. Turk, M. Sandelic, G. Noto, J. R. Pillai, and S. K. Chaudhary, "Primary frequency regulation supported by battery storage systems in power system dominated by renewable energy sources," *J. Eng.*, vol. 2019, no. 18, pp. 4986–4990, Jul. 2019, doi: 10.1049/joe.2018.9349.

[33] P. M. Anderson and M. Mirheydar, "A low-order system frequency response model," *IEEE Trans. Power Syst.*, vol. 5, no. 3, pp. 720–729, Mar. 1990, doi: 10.1109/59.65898.

[34] H. J. Kunisch, K. G. Kramer, and H. Dominik, "Battery energy storage another option for load-frequency-control and instantaneous reserve," *IEEE Power Eng. Rev.*, vols. PER–6, no. 9, pp. 24–25, Sep. 1986, doi: 10.1109/MPER.1986.5527651.

[35] M. R. Aghamohammadi and H. Abdolahinia, "A new approach for optimal sizing of battery energy storage system for primary frequency control of islanded microgrid," *Int. J. Electr. Power Energy Syst.*, vol. 54, pp. 325–333, Jan. 2014, doi: 10.1016/j.ijepes.2013.07.005.

[36] A. G. M. B. Mustayen, M. G. Rasul, X. Wang, M. Negnevitsky, and J. M. Hamilton, "Remote areas and islands power generation: A review on diesel engine performance and emission improvement techniques," *Energy Convers. Manage.*, vol. 260, May 2022, Art. no. 115614, doi: 10.1016/j.enconman.2022.115614.

[37] J. Zhao, X. Lyu, Y. Fu, X. Hu, and F. Li, "Coordinated microgrid frequency regulation based on DFIG variable coefficient using virtual inertia and primary frequency control," *IEEE Trans. Energy Convers.*, vol. 31, no. 3, pp. 833–845, Sep. 2016, doi: 10.1109/TEC.2016.2537539.

[38] M. Fotopoulou, P. Pediaditis, N. Skopetou, D. Rakopoulos, S. Christopoulos, and A. Kartalidis, "A review of the energy storage systems of non-interconnected European islands," *Sustainability*, vol. 16, no. 4, p. 1572, Feb. 2024, doi: 10.3390/su16041572.

[39] M. Asad, S. Martinez, and J. A. Sanchez-Fernandez, "Diesel governor tuning for isolated hybrid power systems," *Electronics*, vol. 12, no. 11, p. 2487, May 2023, doi: 10.3390/electronics12112487.

[40] R. P. Sinha and R. Balaji, "A mathematical model of marine diesel engine speed control system," *J. Inst. Eng. (India), Ser. C*, vol. 99, no. 1, pp. 63–70, Feb. 2018, doi: 10.1007/s40032-017-0420-8.

[41] D. Ochoa and S. Martinez, "Fast-frequency response provided by DFIG-wind turbines and its impact on the grid," *IEEE Trans. Power Syst.*, vol. 32, no. 5, pp. 4002–4011, Sep. 2017, doi: 10.1109/TPWRS.2016.2636374.

[42] V. Y. Singarao and V. S. Rao, "Frequency responsive services by wind generation resources in United States," *Renew. Sustain. Energy Rev.*, vol. 55, pp. 1097–1108, Mar. 2016, doi: 10.1016/j.rser.2015.11.011.
[43] A. S. Ahmadyar and G. Verbic, "Control strategy for optimal participation of wind farms in primary frequency control," in *Proc. IEEE Eindhoven PowerTech*, Jun. 2015, pp. 1–6, doi: 10.1109/PTC.2015.7232290.
[44] L. Xiong, S. Yang, P. Li, S. Huang, C. Wang, and J. Wang, "Discrete specified time consensus control of aggregated energy storage for load frequency regulation," *Int. J. Electr. Power Energy Syst.*, vol. 123, Dec. 2020, Art. no. 106224, doi: 10.1016/j.ijepes.2020.106224.
[45] C. Brivio, S. Mandelli, and M. Merlo, "Battery energy storage system for primary control reserve and energy arbitrage," *Sustain. Energy, Grids Netw.*, vol. 6, pp. 152–165, Jun. 2016, doi: 10.1016/j.segan.2016.03.004.
[46] D. Kottick, M. Blau, and D. Edelstein, "Battery energy storage for frequency regulation in an island power system," *IEEE Trans. Energy Convers.*, vol. 8, no. 3, pp. 455–459, Nov. 1993, doi: 10.1109/60.257059.
[47] M. Benini, S. Canevese, D. Cirio, and A. Gatti, "Battery energy storage systems for the provision of primary and secondary frequency regulation in Italy," in *Proc. IEEE 16th Int. Conf. Environ. Electr. Eng. (EEEIC)*, Jun. 2016, pp. 1–6, doi: 10.1109/EEEIC.2016.7555748.
[48] D. I. Jones, S. P. Mansoor, F. C. Aris, G. R. Jones, D. A. Bradley, and D. J. King, "A standard method for specifying the response of hydroelectric plant in frequency-control mode," *Electr. Power Syst. Res.*, vol. 68, no. 1, pp. 19–32, Jan. 2004, doi: 10.1016/S0378-7796(03)00152-4.
[49] *GE Energy 1.5MW Wind Turbine*. Accessed: Jun. 1, 2023. [Online]. Available: https://geosci.uchicago.edu/~moyer/GEOS24705/Readings/GEA14954C15-MW-Broch.pdf
[50] S. G. Karad, R. Thakur, M. A. Alotaibi, M. J. Khan, H. Malik, F. P. G. Márquez, and M. A. Hossaini, "Optimal design of fractional order vector controller using hardware-in-loop (HIL) and opal RT for wind energy system," *IEEE Access*, vol. 12, pp. 35033–35047, 2024, doi: 10.1109/ACCESS.2024.3357504.
[51] E. Buraimoh and I. E. Davidson, "Laboratory procedure for real-time simulation experiment of renewable energy systems on OPAL-RT digital simulator," in *Proc. 10th Int. Conf. Smart Grid (icSmartGrid)*, Jun. 2022, pp. 221–226, doi: 10.1109/icSmartGrid55722.2022.9848570.
[52] X. Song, H. Cai, T. Jiang, T. Sennewald, J. Kircheis, S. Schlegel, L. N. Martinez, Y. Benzetta, and D. Westermann, "Research on performance of real-time simulation based on inverter-dominated power grid," *IEEE Access*, vol. 9, pp. 1137–1153, 2021, doi: 10.1109/ACCESS.2020.3016177.

MUHAMMAD ASAD received the B.Sc. degree in electrical engineering from the University of Engineering and Technology, Lahore, Pakistan, in 2016, and the M.S. degree in electrical engineering from the University of Gujrat, Gujrat, Pakistan, in 2020. He is currently pursuing the Ph.D. degree in electrical and electronics engineering from the Universidad Politécnica de Madrid, Madrid, Spain. His research interests include electrical power networks, including ancillary services using FACTS devices, and generation and integration of renewable energy sources.

GIULIA TRESCA (Member, IEEE) received the B.Sc. degree in electrical engineering from the University of L'Aquila, L'Aquila, Italy, in 2015, and the M.Sc. and Ph.D. degrees in electrical engineering from the University of Pavia, Pavia, Italy, in 2017 and 2023, respectively. From 2017 to 2019, she was a Test Engineer with Infineon, Villach, Austria. Since 2023, she has been a Research Fellow with PELAB—Power Electronics Group, University of Pavia. Her research interests include multilevel and reconfigurable converters for automotive applications, battery management systems, and control of electrical drives.

PERICLE ZANCHETTA (Fellow, IEEE) received the M.Eng. degree in electronic engineering and the Ph.D. degree in electrical engineering from the Technical University of Bari, Bari, Italy, in 1993 and 1997, respectively. In 1998, he became an Assistant Professor in power electronics at the Technical University of Bari. In 2001, he was a Lecturer with the PEMC Research Group, University of Nottingham, Nottingham, U.K., where he was a Professor in control and power electronics, in 2013. Since 2022, he has been a Full Professor of power electronics with the University of Pavia, Pavia, Italy, and a part-time Professor with the University of Nottingham. He has authored or co-authored more than 400 peer-reviewed scientific articles. His research interests include control and optimization of power converters and drives, and matrix and multilevel converters. He is a member of the Board of Directors of the IEEE Industry Application Society and has been the Editor-in-Chief of IEEE Open Journal of Industry Applications, since 2020. Since 2023, he has been an IEEE-IAS Education Department Chair. He has been the Vice-Chair and the Chair of the IEEE IAS Industrial Power Conversion Systems Department, from 2018 to 2021, and a Secretary, the Vice Chair, and the Chair of the IEEE IAS Industrial Power Converters Committee, from 2012 to 2017.

JOSE ANGEL SANCHEZ-FERNANDEZ (Senior Member, IEEE) received the master's and Ph.D. degrees in civil engineering from the Universidad Politécnica de Madrid, in 1986 and 1995, respectively. He has been an Associate Professor of electrical engineering at the Universidad Politécnica de Madrid (UPM), since 1996, where he has been a Full Professor, since 2025. He has been the Head of the Hydraulic, Energy and Environmental Engineering Department, from 2008 to 2022. His current research interests include grid integration of non-manageable generation, measurement systems, and energy efficiency.